博士論文（要約）

Doctoral Thesis (Abridged)

Multiple myeloma in a murine syngeneic model: fibrinolytic factors during disease progression

(多発性骨髄腫の疾患モデルの作製と

血液線維素溶解系因子群の動態解析)

イアムブンサート　サリタ

CONTENTS

ABBREVIATIONS

MM	Multiple myeloma
BM	Bone marrow
Ig	Immunoglobulin
M protein	Monoclonal protein
ECM	Extracellular matrix
uPA	Urokinase-type plasmin activator
tPA	Tissue-type plasmin activator
PAI	Plasmin activator inhibitor
MMP	Matrix metalloproteinase
uPAR	urokinase plasminogen activator receptor
MT1-MMP	Membrane-type 1 MMP
TNF-α	Tumor necrosis factor-α
IL	Interleukin
bFGF	Basic fibroblast growth factor
VEGF	Vascular endothelial growth factor
TGF	Transforming growth factor
IGF	Insulin like growth factor
TRANCE	Tumor necrosis factor-related activation-induced cytokine
TRAP	Tartrate-resistant acid phosphatase
suPAR	soluble uPAR
YO-2	Trans-4-Aminomethylcyclohexanecarbonyl-Tyr (O-Pic)-octylamide
Plm	Plasmin
Plg	Plasminogen
TA	Tranexamic acid
DMSO	Dimethyl Sulphoxide
ROI	Region of interest
PAP	Plasmin-antiplasmin complex

ABSTRACT

Multiple Myeloma (MM) is a cancer formed by malignant plasma cells, which is characterized by uncontrolled proliferation of abnormal plasma cells in the bone marrow (BM). This disease is treatable but still incurable. The recurrence of the disease is often observed. Therefore, a more effective treatment is still desirable. The fibrinolytic system, which is known to prevent blood clot, has been linked to cancer growth including MM. Main players of the fibrinolytic system are plasminogen-plasmin. Recently, urokinase plasminogen activator (uPA) and its receptor have been identified as predictors for poor prognosis in MM. We hypothesize that the serine plasmin plays a role in MM cell growth and/or dissemination. In this study, we established a murine syngeneic mouse MM model by using CBF1 mouse injected with the murine B53 cells. Mice showed increased circulating plasmin levels, an indicator for the activation of the fibrinolytic system. Treatment with the plasmin inhibitor YO-2 and tranexamic acid was unable to control MM growth *in vivo*. In contrast to the *in vivo* failure of YO-2 to control myeloma cell growth, YO-2 inhibited myeloma cell growth *in vitro* by inducing apoptosis. In conclusion, although plasmin inhibition controlled MM cell growth *in vitro*, the tumor suppressive effect of plasmin inhibitor treatment was not observed *in vivo*.

INTRODUCTION

(I) MULTIPLE MYELOMA

Multiple Myeloma (MM) is a cancer that is caused by malignant plasma cells (a terminal stage of B cell). It is characterized by uncontrolled proliferation of abnormal plasma cells in the bone marrow (BM). MM is the second most common hematological malignancy taking 13% of hematologic cancers and 1% of neoplastic disease [1, 2]. Despite its long recognition since 1844, MM is still incurable [3]. The expected survival period of patients is approximately 4-6 years depending on the disease state and treatment [2]. Novel drugs such as the immunomodulatory drug thalidomide, proteasome inhibitor bortezomib or cellular treatment strategies (e.g., BM transplantation) have been developed to serve as therapeutic strategies for MM. However, these treatment options are often not suitable for all patients due to age limitation. In spite of various options of treatments, recurrence of the disease is still a very common clinical burden. More effective treatment is still desirable.

The main clinical features of MM disease are the accumulation of monoclonal malignant plasma cells within the BM. This accumulation consequently reduces the production of blood cells. For example, in MM patients the decrease in red blood cells can cause anemia, while the reduction of the white blood cells can cause symptoms of immune impairment and increased susceptibility of infection [4]. MM also causes the overproduction of monoclonal immunoglobulin (Ig) or M-protein from the malignant myeloma cell clone. The release of M-protein into the blood circulation and/or into urine can lead to a blood hyperviscosity syndrome with renal failure. The levels of M-protein can be used to follow the disease development. Due to an imbalance between bone resorption and bone formation, patients often suffer from bone pain especially in the backs or ribs [5], and show signs of hypercalcemia. In the late stage of tumor progression, tumor cell spreading also occurs in extramedullar tissues or the peripheral blood [5, 6].

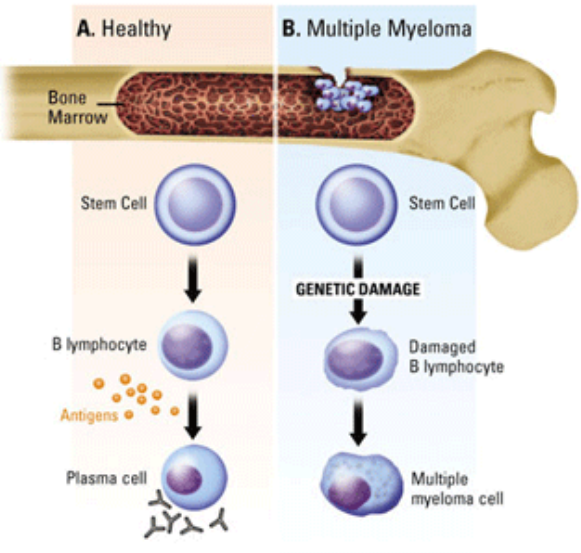

Figure 1: MM development (taken from the website "Disease Overview Booklet Multiple Myeloma Research Foundation Norwalk,CT", http://www.biographicsweb.com/illustration.htm)

The BM microenvironment (niche) in MM

The BM microenvironment is composed of cellular and non-cellular compartments. The cellular compartment includes stromal, endothelial, hematopoietic cells, osteoclasts and osteoblasts, while the non-cellular compartment comprises extracellular matrix (ECM) proteins, oxygen concentration, cytokines, chemokines, etc. [7]. Among these factors, stromal cells are crucial for MM cell survival as they provide essential growth factors and anti-apoptotic factors. Recently, stromal cells have been associated with the resistance to anti-MM chemotherapeutic drug treatment [8, 9].

(II) THE FIBRINOLYTIC SYSTEM

Fibrinolytic factors are well known for blood clot dissolution. The main players in this system are the serine proteases plasminogen and plasmin. Plasminogen (Plg) can be converted into plasmin by the urokinase-type and tissue-type plasminogen activators (uPA and tPA) and kallikrein. The activity of uPA and tPA is controlled by their endogenous inhibitors, the plasminogen activator inhibitor (PAI)-1 and -2. Plasmin (Plm) can convert other downstream proteolytic enzymes (e.g. matrix metalloproteinase (MMP) -2 and -9) [10] from their latent state into their active state. While the proteolytic action of tPA is thought to occur in the blood circulation, uPA's action is believed to occur locally on the cell surface after binding to the uPA receptor, uPAR. The fibrinolytic cascade is shown in Figure 1.

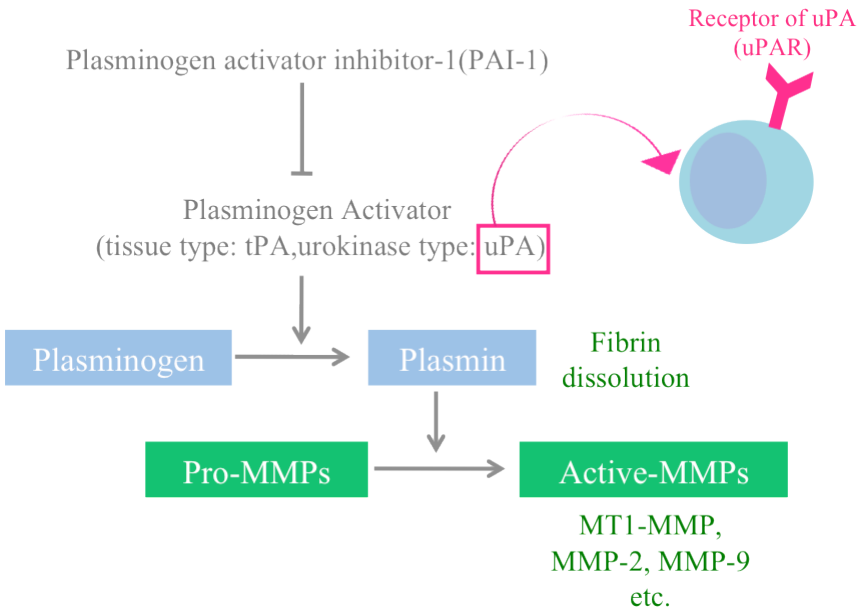

Figure 2: The fibrinolytic system

Components of the fibrinolytic system are not only involved in blood clot dissolution, but also participate in other biological processes including tumor growth, invasion and metastasis. Some of the tumor-related well-known components are mentioned in the next section.

(III) MM AND THE FIBRINOLYTIC SYSTEM

MM cells engage in complex interactions with other cell types like stromal and endothelial cells. These cellular interactions are mediated by various cytokines, which help to promote myeloma cell survival and proliferation in the BM microenvironment, and also support the pathogenesis in this disease. The adherence of myeloma cells to BM stromal cells leads to the overproduction of growth factors that enhance the survival and growth of myeloma cells [11].

Various studies indicate a correlation between the MM disease severity and the fibrinolytic system. Fibrinolytic factors like uPA and its receptor uPAR have been shown to be expressed on primary MM cells [6]. One of the tPA receptors, Annexin A2 which is highly expressed in MM cells, can activate plasmin [12, 13] and is involved in proliferation, apoptosis, invasion and angiogenesis [14]. Not only MM cells, but also *stromal cells within the BM microenvironment* can secrete proteases like matrix metalloproteinases (MMPs) and/or uPA [6]. MMP activation can be facilitated by plasmin [15]. While MM cells express MMP-2, stromal cells have been shown to express MMP-1 and MMP-2. MMP-1 is induced **in stromal cells** after interleukin (IL)-1β, tumor-necrosis factor (TNF)-α and oncostatin M treatment. These cytokines and growth factors can facilitate survival and growth of MM cells [16-18]. Moreover, endothelial cells isolated from MM patients also express MMP-2 and-9 [19].

<u>Tumor growth and proliferation and angiogenesis</u>

Plm can activate cytokine/cytokine receptors like vascular endothelial growth factor-A (VEGF-A), basic fibroblast growth factor (bFGF, also called FGF-2), transforming growth factor-β (TGF-β) and insulin like growth factor-1 (IGF-1). These growth factors support MM growth and promote angiogenesis [20-23]. Plm also can modulate MMPs. MMPs are are zinc-dependent proteinases, which are involved in angiogenesis by ECM remodeling, EC migration and release of angiogenic factors from ECM [24]. For example, MMP-9 released matrix-bound VEGF-A can bind to its receptor causing neoangiogenesis [25]. In addition, MMPs can release the ECM-bound growth factors or even proteolytically activate latent form of some growth factors and cytokines [16, 26].

Osteolysis

When stromal cells adhere to MM cells, stromal cells secrete IL-1β, IL-6, and TNF-β [27]. These factors can prompt stromal cells and osteoblasts to secrete tumor necrosis factor-related activation-induced cytokine (TRANCE), which is involved in osteoclast stimulation. The increased osteoclastic activity causes (1) the release of cytokines like TGF-β, IL-6, bFGF and IGF-1 from the bone matrix, which can stimulate MM growth and (2) causes the release of parathyroid-hormone-related protein. In turn, this protein can activate stromal cells to secrete more TRANCE leading to a vicious cycle between bone resorption and MM growth.

MMPs are one of the key enzymes for bone resorption by osteoclast [28]. The two gelatinases MMP-9 and MMP-2 are produced by osteoclasts and osteoblasts respectively. They can enhance bone degradation in the BM. When MM cells infiltrate into BM, MM-derived MMP-2 and -9 promote osteolysis [5]. In the presence of myeloma cells, osteoblasts can upregulate MMPs and uPA [29], whereas osteoclasts can produce tartrate-resistant acid phosphatase (TRAP), cathepsin K, MMP-1 and -9, and uPA [28]. This accumulating evidence indicates that fibrinolytic factors in part through the activation of MMPs might contribute to MM pathogenesis by altering molecules that modulate MM growth, osteolysis, angiogenesis, MM cell homing and invasion.

Tumor invasion

MMPs play a critical role in homing and invasion in MM [5]. Primary myeloma cells have been reported to express both uPA and the uPA receptor (uPAR or CD87) [30]. Proteolysis of uPAR by uPA or MMP-12 produces a cleaved form of uPAR, the so-called *soluble uPAR (suPAR)*, resulting in the inability of uPA and vitronectin to bind to uPAR [31, 32]. This reveals the possibility that myeloma cell adhesion and invasive properties might be affected by suPAR [33]. The increased level of uPAR and suPAR were suggested as a predictor for poor prognosis and extramedullar involvement in MM patients [30]. Increased suPAR level also correlates with a known predictor for disease progression, for example, disease stages, creatinine, sCD138 [34], and beta2-microglobulin. suPAR can regulate cancer cell infiltration to the BM and other organs.

Among the various types of MMPs, MMP-2 and MMP-9 are the most studied in MM invasion. In MM patients, the increased production of MMP-2 and -9 is associated with tumor progression and MM cell homing to the BM [35]. For other MMPs, it is found that MMP-1 inhibition resulted in the reduction of tumor burden in MM mouse model [5]. Dexamethasone, a frequently used drug in MM patients downregulates MMP-1 expression but it cannot prevent MMP-2 and MMP-9 activation [5, 16, 35-38].

Based on accumulating literature, we hypothesized that the fibrinolytic system is involved in MM progression through MMPs, one of its downstream products.

Clinical symptoms observed in MM patients are linked to the fibrinolytic system. Hypercoagulability is often found in MM patients [39]. MM patients have a high risk of venous thromboembolism. Certain anti-MM chemotherapeutic drugs have been shown to increase the risk of thrombosis in MM patients during the treatment. However, the proteasome inhibitor bortezomib, alone or in combination with other drugs did not increase venous thromboembolism risk [40].

Under steady state conditions, our body keeps a hemostatic balance between thrombosis (blood clotting) and fibrinolysis (blood clot dissolution) to maintain homeostasis. An increase in fibrinolytic factors has been detected in clinical samples of patients with MM during disease progression and after thrombosis had occurred.

We hypothesize that the fibrinolytic system, and here specifically its main players **plasminogen-plasmin** are increased/activated during disease progression. Many studies demonstrated the involvement of MMPs in the pathogenesis of MM and other types of cancers. Therefore, MMP inhibitors have been explored as anti-cancer treatments, but were withdrawn from clinical studies as severe side effects occurred in MMP inhibitor-treated patients. This gives room for the exploration of potential other upstream targets, like plasmin. Recently, we reported that genetic plg deficiency and pharmacological plm inhibition reduced tumor growth in murine T-cell lymphoma models by suppressing MMP-9 dependent $CD11b^{+}/F4/80^{+}$ myeloid cell recruitment into tumors, and the local release of myeloid cell derived cytokines [41]. This study also demonstrated that plasmin inhibition could prevent the activation of MMPs.

In this study, we investigated whether plm inhibition can prevent the progression of MM. Given the controversy of fibrinolytic system in MM [39], we first investigated the expression pattern of fibrinolytic factors in MM cells and other cells known to contribute to MM cell niche, the stromal cells *in vitro*. We further determined the dynamics of the activation of the fibrinolytic system *in vivo*. In addition, we tested the effects of two plm inhibitors for MM growth: the direct plm inhibitor, YO-2, and indirect plm inhibitor, tranexamic acid. The details of these 2 compounds are explained in the following sections.

<u>YO-2</u>

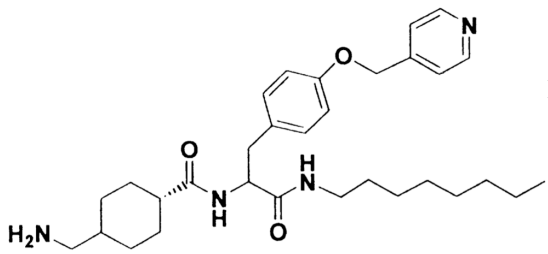

Figure 3: The structure of YO-2 [42]

Trans-4-Aminomethylcyclohexanecarbonyl-Tyr (O-Pic)-octylamide (YO-2) is a newly developed plm inhibitor. YO-2 can bind directly to the active site of plm after being converted from plg by PAs. YO-2 prevents tumor growth in part by inducing apoptosis in solid tumors like the M1 melanoma cell line and human HT29 colon carcinoma cell line through activation of caspase-3 [42]. Others reported that the anti-tumor effect of YO-2 is mediated by its ability to inhibit proteases [43]. Due to the success in inhibition of solid tumors and T cell lymphoma, one of the hematological malignancies, we decided to test the activity of YO-2 to control MM cell proliferation/growth *in vitro* and *in vivo*.

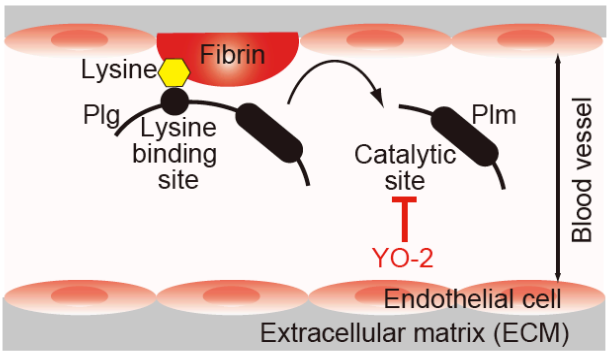

Figure 4: YO-2 blocks the catalytic site of plm [44].

Tranexamic acid (TA)

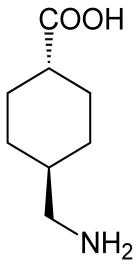

Figure 5: The structure of tranexamic acid

T

A can indirectly inhibit plm by blocking the lysine-binding site on the plg molecule to reduce its binding affinity to fibrin causing the decrease of plg activation [45]. TA is in clinical use for patients to control excessive bleeding e.g. after tooth extraction, surgery, etc. [46]. TA inhibited tumor metastasis of Lewis lung carcinoma cell and reduced tumor growth in patients with advanced ovarian cancer and breast cancer. Mechanistically, it was shown that the anti-tumor effect of TA was due to its ability to prevent fibrin dissolution around the tumor, which can interfere with tumor growth [47-49].

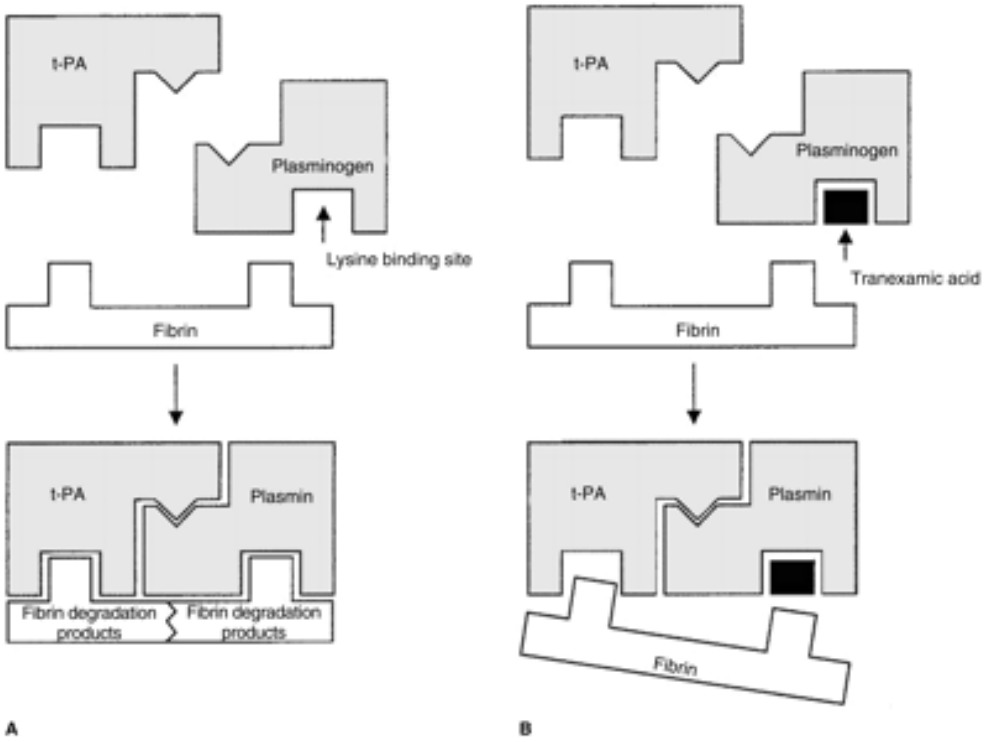

Figure 6: The mechanism of plg inhibition by tranexamic acid (A) Fibrinolytic activation (B) Tranexamic acid blocks the lysine binding site of plg [46].

PURPOSE

Here, we hypothesize that *fibrinolytic factors play a role in MM cell growth* as they either can control the activation of disease-associated proteases like MMPs or can directly modulate other molecular downstream targets (cytokine, receptors or extracellular matrix molecules) involved in MM pathogenesis. The ultimate goal of this project is to determine whether agents inhibiting the function of plm are effective to prevent MM disease progression.

MATHERIAL AND METHODS

REAGENT

YO-2

The plasmin inhibitor YO-2 [*trans*-4-aminomethylcyclohexanecarbonyl- Tyr(*O*-Pic)-octylamide] was kindly provided by Yoshio Okada (Kobe Gakuin University, Kobe, Japan) [50, 51]. Its molecular weight is 595.63 g/mol.

In vivo: YO-2 was dissolved in PBS or 0.9%NaCl/DMSO (at a ratio of 9:1) at 375 µg/ml. The solution was prepared by dissolving 15 mg of YO-2 in 40 ml of solvent, referred in this study as a concentration of 1x. When double, three or four times of 1x YO-2 was dissolved, a 2x, 3x or 4x concentration was prepared. YO-2 was intraperitoneally injected daily at a concentration of 3.75 mg/kg per mouse starting on day 0, the first day of cancer inoculation, until the death of mice was observed.

In vitro: YO-2 was dissolved in sterile Dimethyl Sulphoxide (DMSO) at 25 mM as stocking solution before diluting into another desired concentration.

Tranexamic acid (TA)

TA was administered orally. To prepare TA in drink water, 12.5 mg TA (Daiichi-Sankyo) was dissolved in 500 ml sterile water. The drug was administered via drinking water.

Bortezomib

Bortezomib was purchased from Cell Signaling Technology (#2204). Its molecular weight is 384.24 g/mol. It was dissolved in sterile DMSO. For *in vivo* experiments, mice were injected intraperitoneally twice a week at a concentration of 0.25 mg/kg of mouse. Bortezomib was added to *in vitro* cultures at concentrations ranging from 5-100 nM.

Chemotherapeutic drugs

Thalidomide (Fujimoto-seiyaku, Japan, 1009J032), doxorubicin (LC laboratories, US, D-4000) and dexamethasone (Sigma, US, D4902-500MG) were dissolved in sterile DMSO, PBS and ethanol, respectively.

Viviren™ In Vivo Renilla Luciferase substrate

The Viviren was purchased from Promega, USA. The stock solution was made in sterile DMSO at a concentration of 10 μg/μl and kept in -20°C. A working solution was prepared by dissolving the stock solution in PBS at the concentration 0.1 μg/μl of Vivren for injection. 100 μl of the working solution was administered by i.v. injection and luciferase signal was determined immediately after injection

MICE

Animal procedures were performed in accordance with institutional protocols and were approved by the Institutional Animal Care Animal Care and Use Committee of the Institute of Medical Science, The University of Tokyo.

CBF1 mice

CBF1 or CB6F1/Slc (Slc:CBF1, $H2k^{b/d}$) mice were purchased from Japan SLC Inc (Hamamatsu, Japan). 6-8 week-old female mice were used in the experiments. The CBF1 mouse strain is the F1 hybrid between the C57BL/6 and BALB/c mouse strain.

NOD/SCID mice

NOD/SCID or NOD.CB17-Prkdc<scid>/J mice are non-obese diabetic-severe combined immunodeficient mice. 6-8 week-old female mice were used in this experiment.

CELL LINES

Murine B53 Cells

The mouse B-cell B53 is a plasmacytoma cell line (BALB/c origin; H-2^d, kindly provided by Ko Okumura, Juntendo University School of Medicine, Japan), a cell line that produces anti-DNP (dinitrophenyl) IgE antibody [52]. B53 cells were maintained in RPMI-1640 (4,500 mg/l glucose) with L-glutamine, phenol red, HEPES and sodium pyruvate (Wako, Japan) medium containing 10% fetal bovine serum and 1x penicillin/streptomycin (Nacalai Tesque Inc, Japan).

Murine Sp2/0-Ag14 cells

Sp2/0-Ag14 myeloma cells (kindly provided by Hiromitsu Nakauchi, Institute of Medical Science, The University of Tokyo, Japan) were expanded in RPMI-1640 (4,500 mg/l glucose) with L-glutamine, phenol red, HEPES, sodium pyruvate (Wako, Japan) medium containing 10% fetal bovine serum and penicillin/streptomycin.

Human RPMI8226 and MM.1S cells

The RPMI8226 cell line (ATCC® CCL-155™ Lot 60553158) is a plasmacytoma cell line. In some experiments, *Renilla Luciferase labeled RPMI8226* cells, which were kindly provided by Muneyoshi Futami (Institute of Medical Science, The University of Tokyo, Japan), were used for *in vivo* injection. They were cultured in RPMI-1640 (4,500 mg/l glucose) with L-glutamine, phenol red, HEPES and sodium pyruvate (Wako, Japan) medium containing 10% fetal bovine serum and 1x penicillin/streptomycin.

Stromal cell lines

The mouse stromal cell line MS5 and the human stromal cell line HS5 were tested. MS5 cells were cultured in Iscove's Modified Dulbecco's Medium with L-glutamine, phenol red, HEPES and sodium pyruvate (Wako, Japan) containing 10% fetal bovine serum and 1x penicillin/streptomycin.

HS5 cells (purchased from ATCC® CRL-1182) were cultured in DMEM (High glucose) with L-glutamine and phenol red (Wako, Japan) containing 10% fetal bovine serum and 1x penicillin/streptomycin.

CELL CYTOTOXIC ASSAY

To determine the cytotoxicity of YO-2, the human MM RPMI8226 cells (1 x 10^5 cells/1ml/well) and the mouse hybridoma B53 cells (1 × 10^5 cells/1ml/well) were cultured in triplicate in the presence of different concentrations of YO-2 or in 0.2% DMSO for 24 hours. Trypan blue exclusion test was used to determine the cell viability and indicate the percentage of 50% inhibitory concentration (IC_{50}). The YO-2 concentration that induced cell death in 50% or more of myeloma cells was used in cultures of primary cultured cells (splenocytes and bone marrow mononucleated cells retrieved from C57/BL6 mice) and the non-malignant cell lines, THP-1 (human monocytic cell line) and RAW264.7 (murine macrophage cell line). The chemosensitivity of cultured B53 cells for bortezomib, thalidomide, doxorubicin and dexamethasone of B53 cells was tested after 24 hours of incubation. Appropriate controls for each drug solvent were tested.

DRUG SENSITIVITY TESTING IN VITRO

Human RPMI8226 (1 x 10^5 cells/well) and mouse hybridoma B53 cells (1 × 10^5 cells/well) were stimulated with 10 and 20 μg/ml of YO-2 in a total volume of 1 ml medium in the presence or absence of bortezomib (5 μM/ml). Cells were cultured in 12-well plates (TPP, Switzerland). After 12 hours, cells were collected and the apoptosis rate was determined using trypan blue exclusion.

CELL APOPTOTIC ASSAY

The cell apoptotic assay was performed according to the manufacturer's protocol (FITC Annexin V Apoptosis Detection Kit I; Cat no. 556547, BD Pharmingen). In brief, B53 or RPMI8226 cells were treated with various anti-myeloma drugs or YO-2 as mentioned above. Collected cells were washed

with cold PBS twice and resuspended at a concentration of 1 x 10^5 cells in 100 µl of 1x Annexin V binding buffer. Cells were stained by FITC-conjugated Annexin V and PI-containing binding buffer for 15 min in the dark at room temperature. After incubation, 400 µl of 1x Annexin V binding buffer was added to each tube. Samples were then analyzed by FACSVerse™ flow cytometry within 1 hour.

In vivo MYELOMA MOUSE MODEL

MM cells were prepared before i.v. or s.c. injection. Briefly, B53 or RPMI8226 cells were collected, washed twice with PBS, and resuspended in PBS or FBS-free RPMI-1640. To ensure single cell suspension, cells were filtered through a 40 µM nylon strainer (BD Falcon). Cells were counted and prepared at indicated cell concentration. Cell preparations exceeding 90% viability by trypan blue dye exclusion were used in the experiments. For *in vivo* administration of YO-2, MM cell-inoculated mice were injected every other day with YO-2 at a concentration of 3.75 mg/kg body weight.

Intravenous syngeneic B53 model

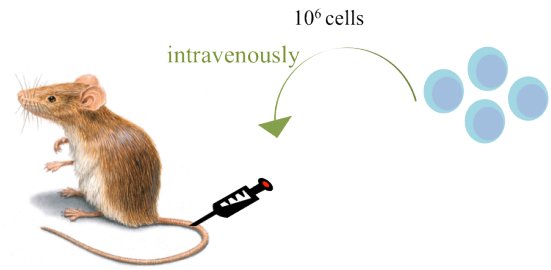

Cell administration: On day 0, CBF1 mice were injected with 10^6 B53 cells/mouse. Cells were inoculated intravenously into 6-8 week-old female CBF1 mice

Figure 7: Murine syngeneic B53 model

Subcutaneous xenograft model

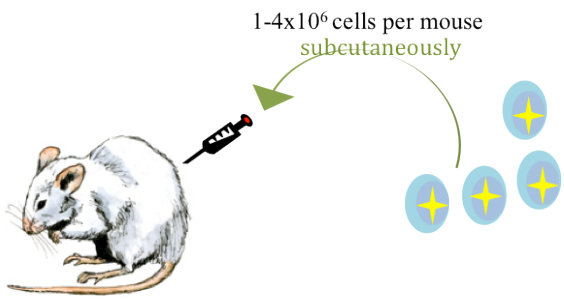

Cell administration: The dorsal skin of mice was shaved one day before tumor cell inoculation (day -1). The following day (day 0), PBS-washed Renilla Luciferase labeled RPMI8226 cells were injected at a concentration of 1 or 4 x 10^6 RPMI8226 cells/mouse subcutaneously into NOD/SCID mice.

Figure 8: Murine xenograft RPBMI8226 model

Tumor load evaluation: Tumor length, width, and height were measured by a vernier caliper and the tumor volume was calculated using the following equation [(length) x $(\text{width})^2$]/2. Moreover, the tumor load was determined by measuring the luciferase signal as mentioned using *in vivo* bioluminescence imaging.

In vivo BIOLUMINESCENCE IMAGING

NOD/SCID mice injected with human RMPI8226 cells s.c. In order to assess tumor burden pre- and post-therapy, tumors were imaged at post-inoculation day 0, 7, 21 and 35. For bioluminescence imaging, mice were anesthetized with isoflurane (Pfizer). Then, they were injected intravenously with 10 µg of Viviren™ In Vivo Renilla Luciferase substrate (Promega, USA). The luciferase signal could be determined immediately after substrate injection. Using an IVIS® Imaging System 100 Series (Xenogen corporation, USA), images were acquired using a ≤60 second exposure time. The luciferase signal intensity was quantified using region of interest (ROI) (total flux, p/s) with Living Image® 2.50.1 software.

BLOOD EXAMINATION AND BONE OSTEOLYSIS

Mice were bled retro-orbitally and plasma samples was taken at indicated time points and stored at -30°C until further analysis. Bone osteolysis was visualized by x-ray of anesthetized mice (n = 3 per group).

SURVIVAL

Mouse survival was monitored on a daily basis. Mice were killed when they showed severe signs of pain, body weight loss >20% when compared to the initial body weight, and/or the tumors reached a size of >2 cm or mice appeared moribund.

ELISA

Anti-DNP IgE antibody (Alpha Diagnostic International), PAP (CUSABIO), total uPA (Innovative Research, Inc), tPA (Innovative Research, Inc), suPAR (Cloud-Clone Corp) and PAI-1 (Molecular Innovations) levels were measured in blood samples using commercially available ELISA kits according to the manufacturer's recommendations.

ORGAN INFILTRATION

Femur, tibiae, spleen and liver tissues were collected to determine MM cell organ infiltration. Spleen and liver were homogenized and pelleted. Femurs were flushed out to determine the total number of BM cells. Collected BM cells were subjected to antibody staining procedures and followed by flow cytometry analysis. Paraffin blocks were prepared from femurs, spleen and liver tissues. BM cells from femur were also used for RNA extraction.

To identify the presence of mouse myeloma cells in the tissues, cells were stained with FITC anti-mouse H2k^{d} (clone SF1-1.1, Biolegend, San Diego, CA), PE anti-mouse H2k^{b} (clone AF6-88.5, BD Pharmingen, USA), and APC anti-mouse CD138 (syndecan-1) (clone 281-2, Biolegend, USA) at 4°C for 30 minutes, according to the manufacturer's protocol. Dead cells were excluded using PI staining. Cells were analyzed using a FACSVerse^{TM} flow cytometry.

HISTOLOGY

Bones (femur), liver and spleen tissues were excised for histological examination and fixed in neutral buffered formaldehyde (4%) overnight at RT. Bones were decalcified in 10% EDTA (pH7.4) for 21 days, until they lost the normal structural rigidity. The bones were then embedded in paraffin blocks and 5 µm section cuts were prepared. Sections were subsequently stained with hematoxylin and eosin (H&E), and analyzed using an upright fluorescence microscope (Olympus Optical Co. Ltd, UK).

RT-PCR

RNA was extracted using TRIzol (Life technology, CA). The purity and integrity of the extracted RNA was analyzed spectroscopically prior to use. cDNA was generated using an High-Capacity cDNA Reverse Transcription Kits (Applied Biosystems, CA, USA) and was stored at –20°C. PCR mixtures (20 µL final volume) contained 10 µl of SYBR green mix (Promega, Heidelberg, Germany), 2 µl of 1 ng/ µl template cDNA and 1 µl of 10 µM primers and 7 µl of water. Reaction mixtures were incubated in a thermocycler. The respective forward and reverse primers used for RT-PCR were as follows:

Table 1: The list of mouse primers

MOUSE PRIMER	SEQUENCES
GAPDH	5'-TCT TGC TCA GTG TCC TTG CTG GG-3' 5'-TGC GAC TTC AAC AGC AAC TCC CAC-3
uPA	5'-GTC CTC TCT GCA ACA GAG TC-3' 5'-CTG TGT CTG AGG GTA ATG CT-3'
tPA	5'-GTA CTG CTG CTT TGT GGA CT-3' 5'-TGC TGT TGG TAA GTT GTC TG-3'
uPAR	5'-TCT GGA TCT TCA GAG CTT TC-3' 5'-AGC ACA TCT AAG CCT GTA GC-3'
PAI-1	5'-AAA GGA CTC TAT GGG GAG AA-3' 5'-TAG GGA GGA GGG AGT TAG AC-3'

Table 2: The list of human primers

HUMAN PRIMER	SEQUENCES
GAPDH	5'-TGG TCT CCT CTG ACT TCA AC-3' 5'-CTG TTG CTG TAG CCA AAT TC-3'
uPA	5'-CCC TCC TCT CCT CCA GAA GAA-3' 5'-GTA GAC GAT GTA GTC CTC CTT C-3'
tPA	5'-GAT GCG AAA CTG AGG CTG GCT GTA CTG TCT C-3' 5'-GGA AGT ACA GCT CAG AGT TCT GCA GCA CCC CTG C-3'
uPA-R	5'-GGT GAC GCC TTC AGC ATG A-3' 5'-CCC ACT GCG GTA CTG GAC AT-3'
PAI-1	5'-CAG ACC AAG AGC CTC TCC AC-3' 5'-ATC ACT TGG CCC ATG AAA AG-3'

STATISTICS

Survival curves were plotted using Kaplan-Meier estimates. Data are reported as the mean ± standard error of the mean (SEM). Student's *t*-test was used for statistical analysis of remaining data. $P < 0.05$ was considered statistically significant.

RESULTS

Stromal, but not most MM cell lines express fibrinolytic factors

Previous reports demonstrated that patient derived myeloma cells express uPA and its cellular receptor uPAR [6]. In contrast to human primary MM cells, most tested human and murine MM cell lines showed no or very low uPA, tPA, uPAR and PAI-1 expression as determined by qPCR (Figure 9 and 10).

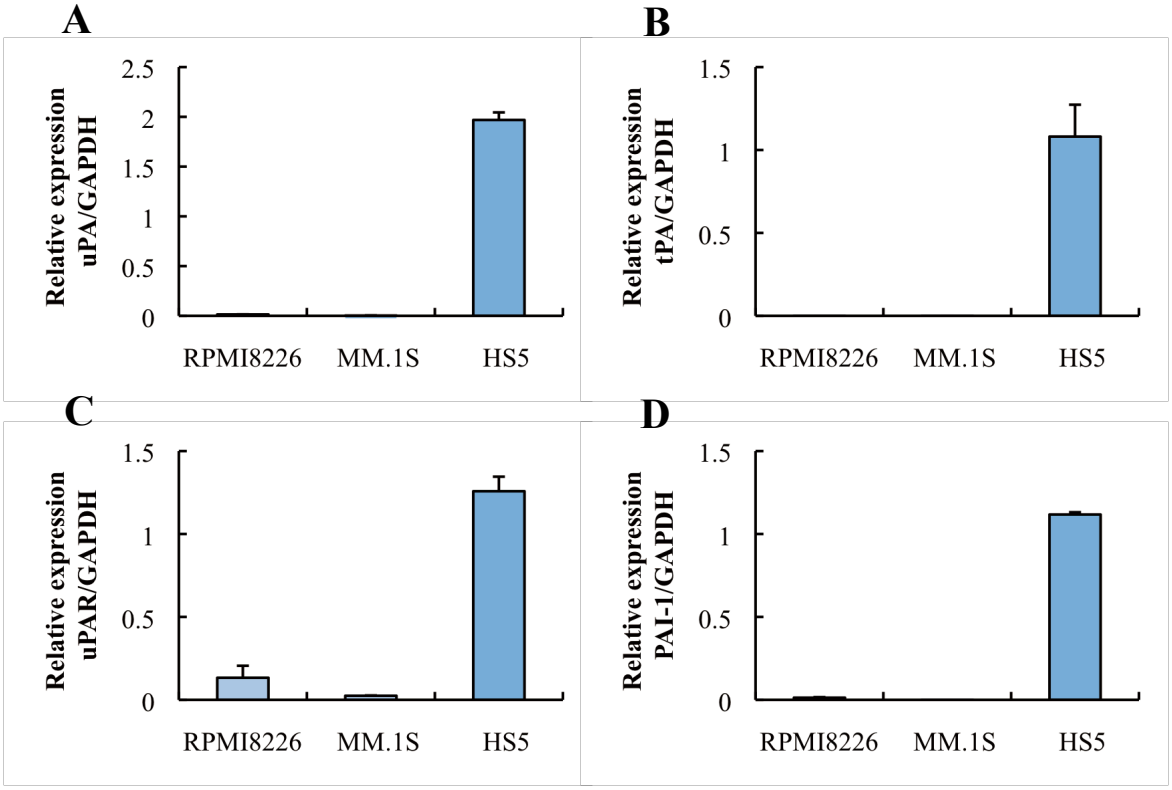

Figure 9: Human stromal rather than myeloma cell lines expressed high levels of fibrinolytic factors. The relative gene expression of **(A)** uPA, **(B)** tPA, **(C)** uPAR and **(D)** PAI-1 on human MM cell lines (RPMI8226, MM.1S), and the human stromal cell line HS5 as determined by qPCR. qPCR was performed where GAPDH served as a reference gene. Each data point was performed in triplicate and each experiment was at least repeated twice. Representative data are shown. Data are represented as mean ± SEM.

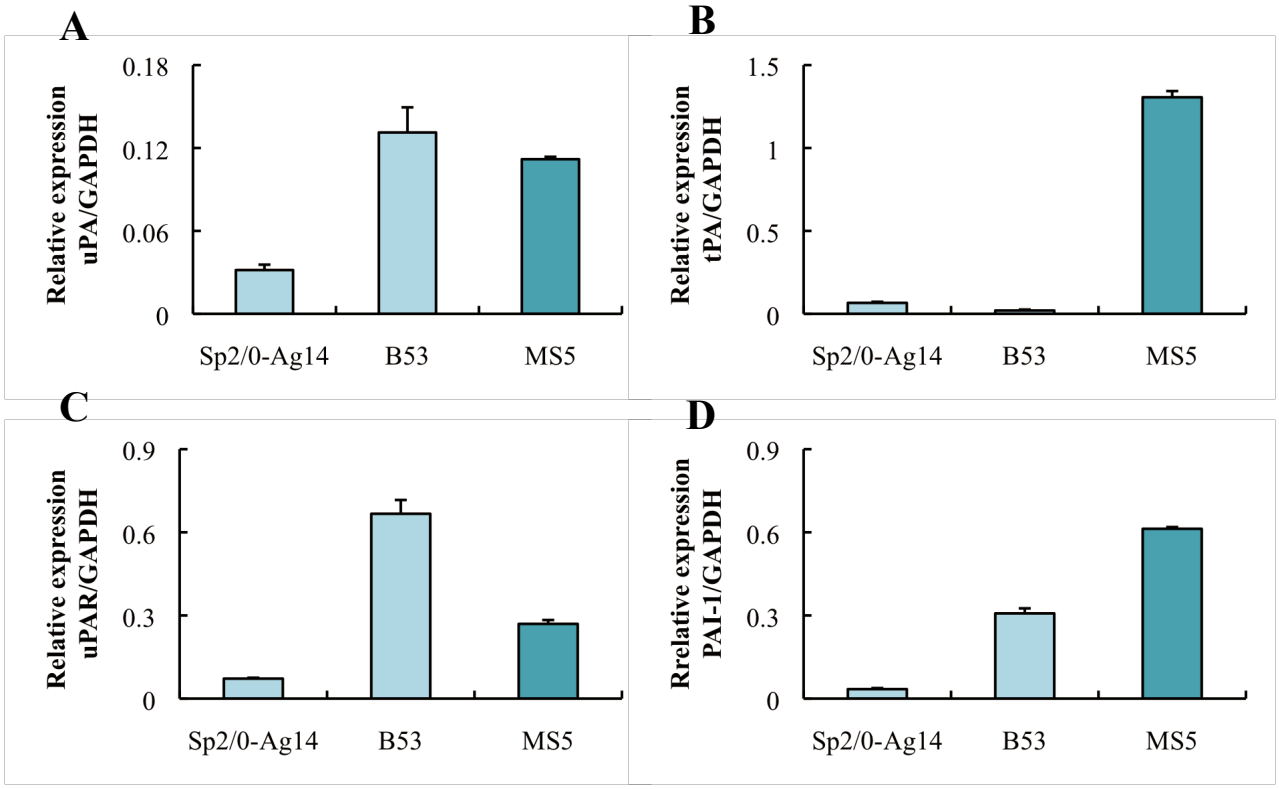

Figure 10: B53 cells showed high expression of uPA and uPAR. The relative gene expression of **(A)** uPA, **(B)** tPA, **(C)** uPAR, and **(D)** PAI-1 was determined on mouse MM cell lines, Sp2/0-Ag14 and B53, and the mouse stromal cell line MS5 by qPCR. qPCR was performed where GAPDH served as a reference gene, and where each data point was performed in triplicate. Each experiment was repeated at least twice and the representative data are shown. Data are represented as mean ± SEM.

The murine plasmocytoma B53, but not the Sp2/0-Ag14 cells showed high uPA and uPAR gene expression (Figure 10). Because MM cell survival is controlled by cell interactions with the ECM and BM stromal cells, and stromal cells are a known source for fibrinolytic factors in other tumors [10], BM stromal cell lines were included in the analysis. In contrast to MM cells, high expression of uPA, tPA, uPAR and PAI-1 was detectable in the human and murine stromal cell lines, HS5 and MS5.

These data suggest that stromal cells are a source of fibrinolytic factors in the BM. Because B53 cells showed an expression pattern for fibrinolytic factors similar to that reported by others of primary human MM cells, this cell line was used for further studies.

Chemosensitivity of the murine B53 MM cell line

B53 and RPMI8226 cells were tested. Both cell lines are murine and human plasmacytoma cell lines, respectively. We studied the chemo-sensitivity of B53 for the MM cell-active drugs bortezomib, thalidomide, dexamethasone and doxorubicin *in vitro*. The IC_{50} of the human cell line RPMI8226 was between 3 to 5 nM for bortezomib (Figure 11B) and around 10 nM for doxorubicin and dexamethasone (Figure 11C and D). The proliferation of murine B53 cells was efficiently blocked after treatment with bortezomib and doxorubin, but B53 cells were unresponsive to thalidomide and dexamethasone (Figure 12). In contrast, RPMI8226 cells showed responsiveness to all MM drugs tested, except for thalidomide. Bortezomib and doxorubicin used as single agents can significantly decrease the numbers of viable B53 cells.

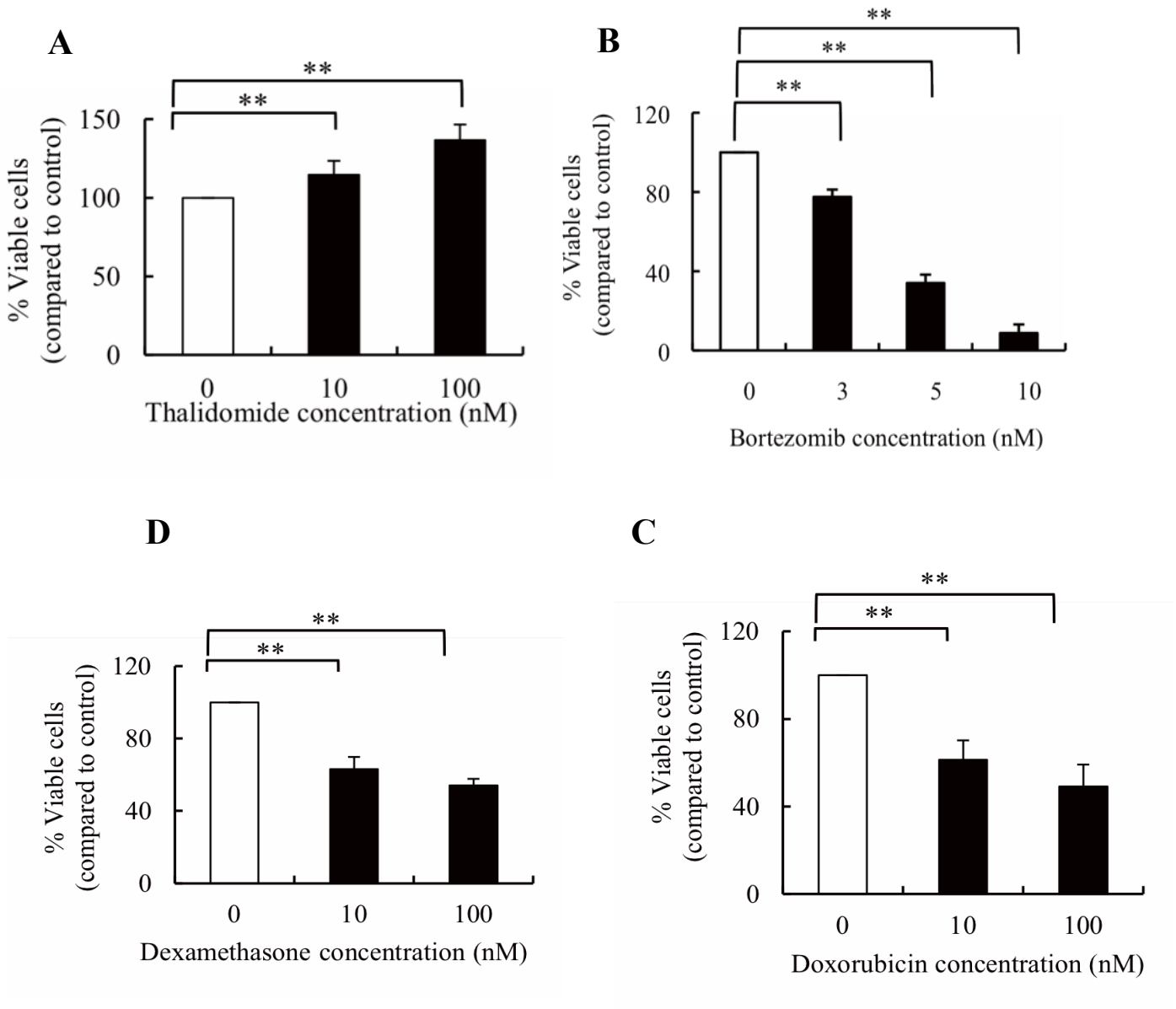

Figure 11: The human RPMI8226 MM cell line responded to common chemotherapeutic drugs except thalidomide. Human RPMI8226 cells were cultured for 24 h in the presence of indicated concentration of **(A)** thalidomide, **(B)** bortezomib, **(C)** doxorubicin and **(D)** dexamethasone. Cell viability was determined via trypan blue exclusion staining. Data are shown as a representative of two independent experiments with similar results. Data are represented as mean ± SEM. $^{**}p \leq 0.02$.

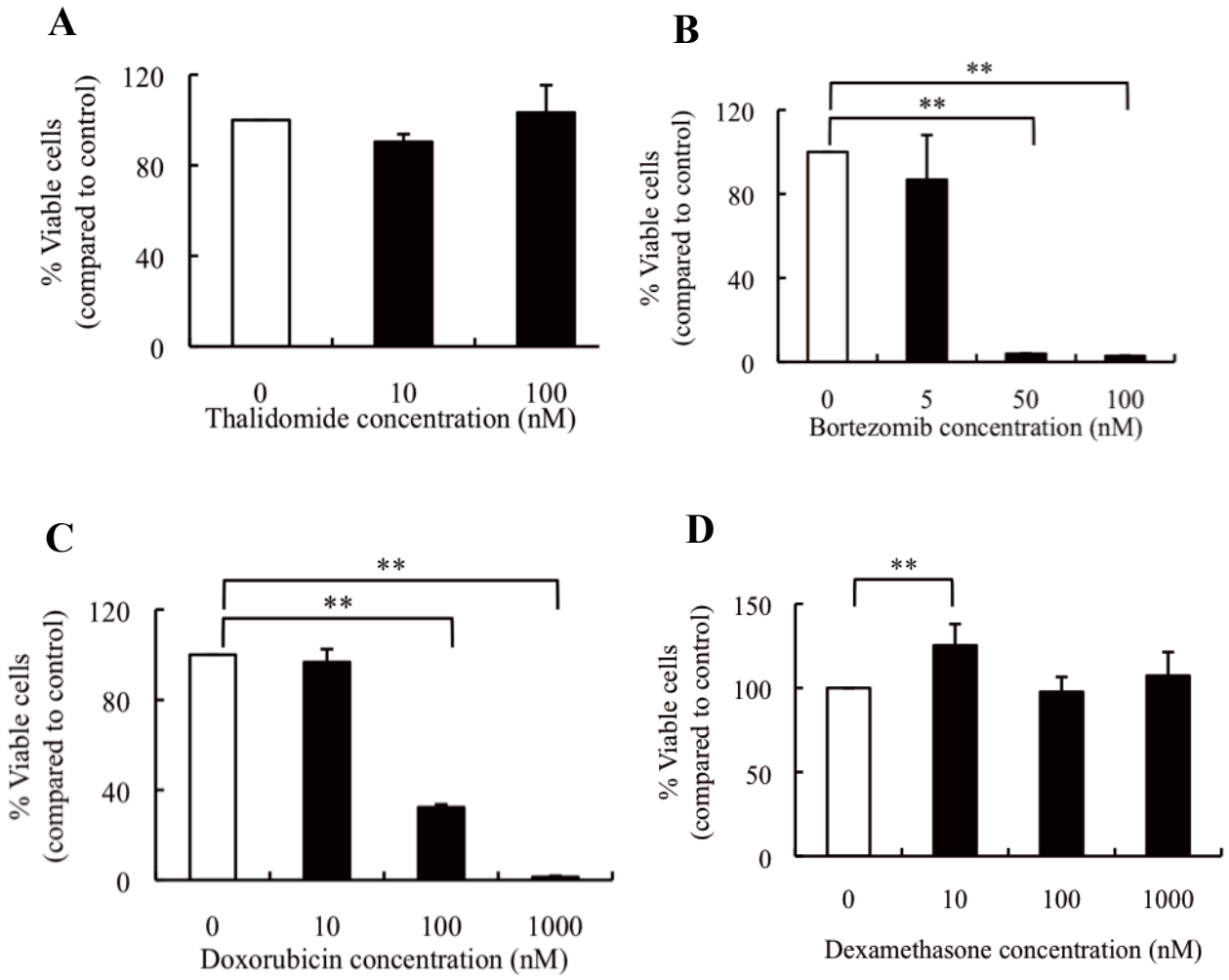

Figure 12: B53 cell line showed responsiveness to the MM-active drugs bortezomib and doxorubicin. The murine B53 cells were cultured in the presence or absence of the common chemotherapeutic drugs, **(A)** thalidomide, **(B)** bortezomib, **(C)** doxorubicin, and **(D)** dexamethasone. Cell viability was determined by trypan blue exclusion staining. Data are shown as a representative of at least two or three independent experiments with similar results. Data are represented as mean ± SEM. $^{**}p \leq 0.02$.

Plm is activated during MM progression in the murine B53 syngeneic MM model

The IgE-secreting B53 hybridoma cells were injected intravenously (i.v.) into CBF1 mice. Given that B53 cells express both uPA and uPAR, which can pericellular result in the activation of plm, we next investigated whether fibrinolytic factors were activated during disease progression in this murine B53 syngeneic MM model.

Higher tPA expression was found in bone marrow mononuclear cells (BMMCs) isolated at day 20 after tumor cell inoculation as compared to BMMCs isolated at day 0 as determined by qPCR (Figure 13B). Increased PAI-1 levels have been reported in patients with newly diagnosed MM [53]. We found increased PAI-1 expression in BMMCs by qPCR (Figure 13A), but no significant change in circulating PAI-1 levels in plasma 20 days after inoculation when compared to plasma from mice before MM cell injection as determined by ELISA (Figure 14B).

It was reported that uPAR is expressed in MM cells derived from MM patients [30]. High levels of soluble uPAR (suPAR) in human MM patient samples predict disease progression and a shortened survival and early extramedullar MM infiltration [30]. suPAR plasma levels in blood circulation slightly increased by day 20 after inoculation (Figure 14A) when compared to non-MM cell-bearing mice. However, no significant difference was observed between YO-2-treated, PBS-treated or normal mice.

Murine plasmin-α2 antiplasmin complex (PAP) plasma levels were increased by day 20 after B53 cell inoculation indicating the activation of fibrinolysis during MM progression (Figure 15). Given that plm activation occurred in the B53 syngeneic MM murine model, we next tested the plm inhibitor YO-2 on modulating fibrinolytic factors *in vivo*. Plm inhibition by YO-2 at a concentration of 1x slightly, but not significantly suppressed PAP levels by day 20 (Figure 15).

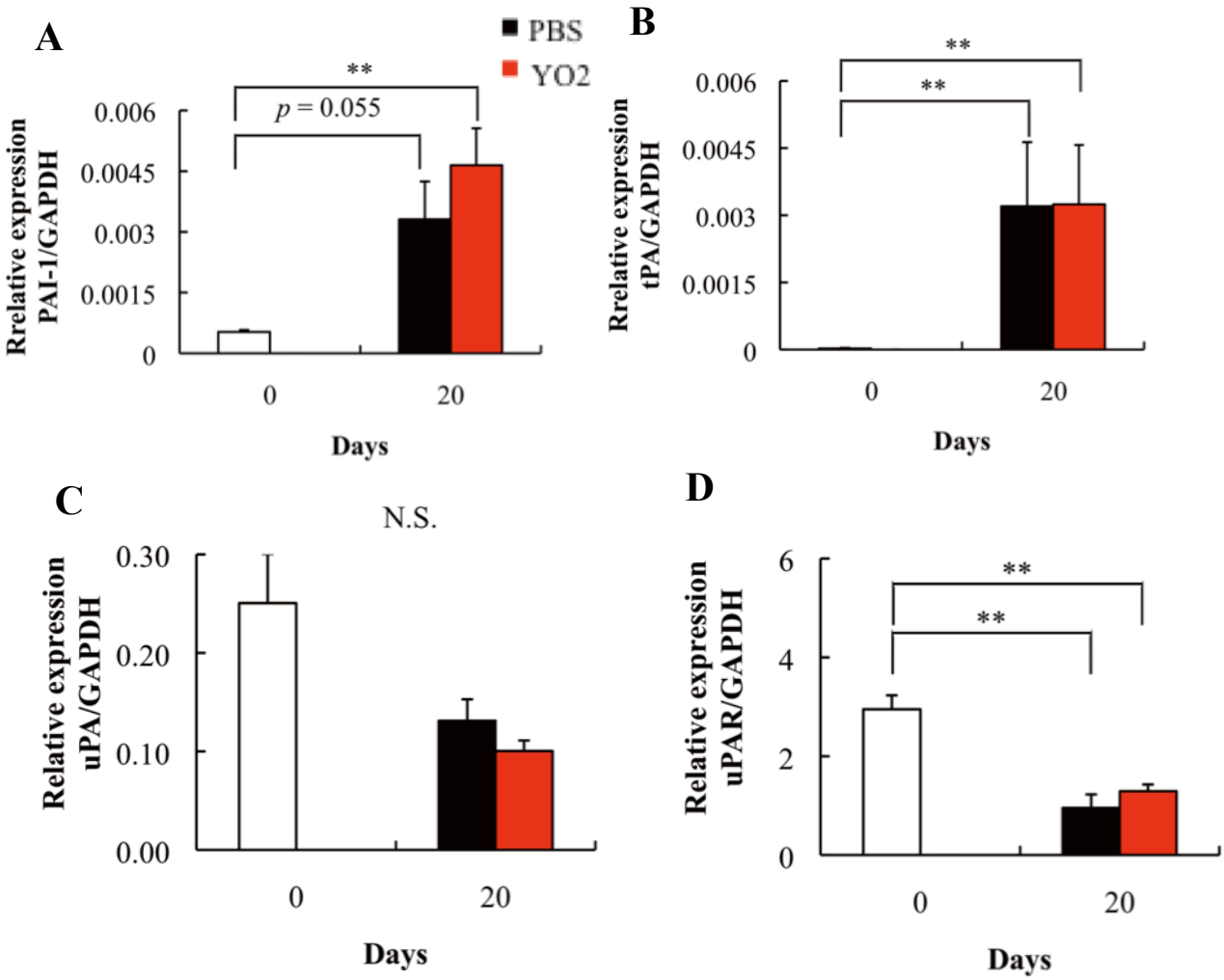

Figure 13: Upregulation of PAI-1 and tPA gene expression in BMMNCs of B53 inoculated mice. CBF1 mice were injected with 1 x 10^6 B53 cells and treated every other day with phosphate-buffered saline (PBS) or YO-2 (i.p. 3.75 mg/kg). 20 days after B53 inoculation into CBF1 mice, BMMCs were collected and extracted for RNA. Gene expression was determined for murine **(A)** PAI-1, **(B)** tPA, **(C)** uPA and **(D)** uPAR. qPCR was performed where GAPDH served as a reference gene, and each data point was performed in triplicate. Data are represented as mean ± SEM. $^{**}p \leq 0.02$.

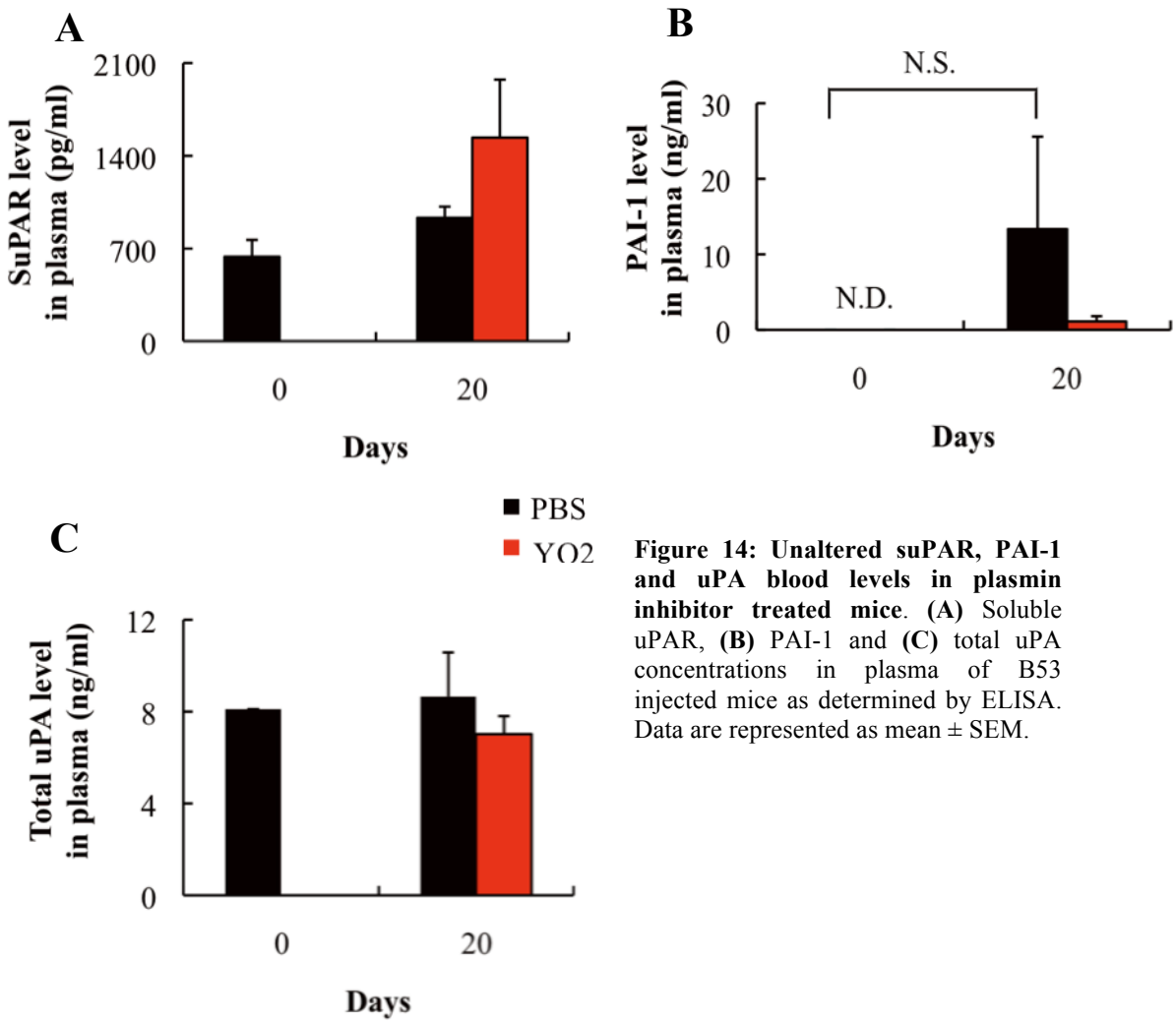

Figure 14: Unaltered suPAR, PAI-1 and uPA blood levels in plasmin inhibitor treated mice. **(A)** Soluble uPAR, **(B)** PAI-1 and **(C)** total uPA concentrations in plasma of B53 injected mice as determined by ELISA. Data are represented as mean ± SEM.

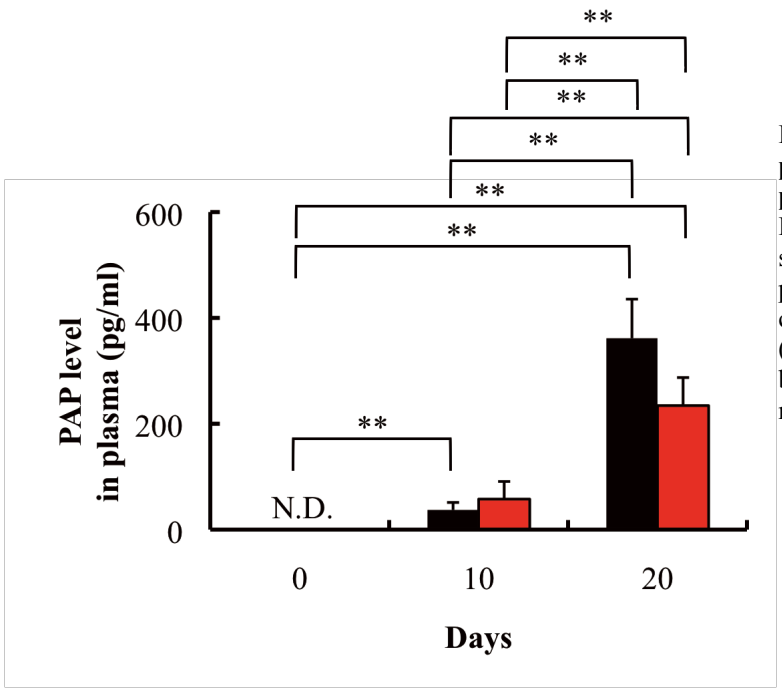

Figure 15: Increased circulating plasmin levels during tumor progression in the murine syngeneic B53 hybridoma model. Plasma samples were collected at indicated time points from mice injected i.v. with B53 cells. Plasmin-α2 antiplasmin complex (PAP) plasma levels were determined by ELISA. n = 8-19 per group. Data are represented as mean ± SEM. $^{**}p \leq 0.02$.

Plm inhibitor treatment does not prevent MM disease progression in the B53 MM model

Next, we tested myeloma cell infiltration in YO-2-treated and PBS-treated mice. Tumor cell infiltration, in part with the formation of large tumor nodules was observed after microscopic analysis of Hematoxylin and Eosin (H&E)-stained BM (Figure 16A), spleen (Figure 16B), and liver sections (Figure 16C) on day 20 after B53 cell injection.

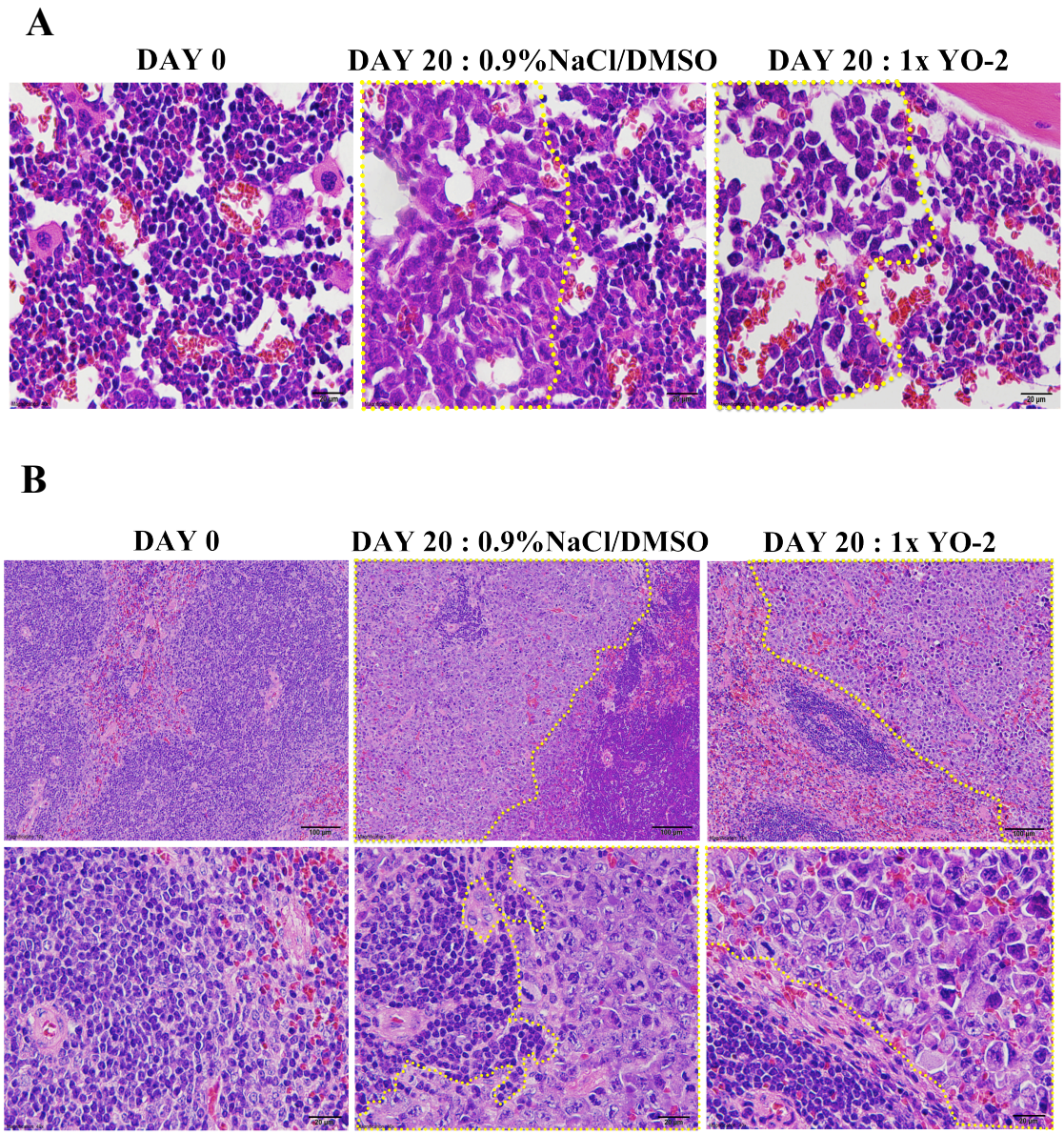

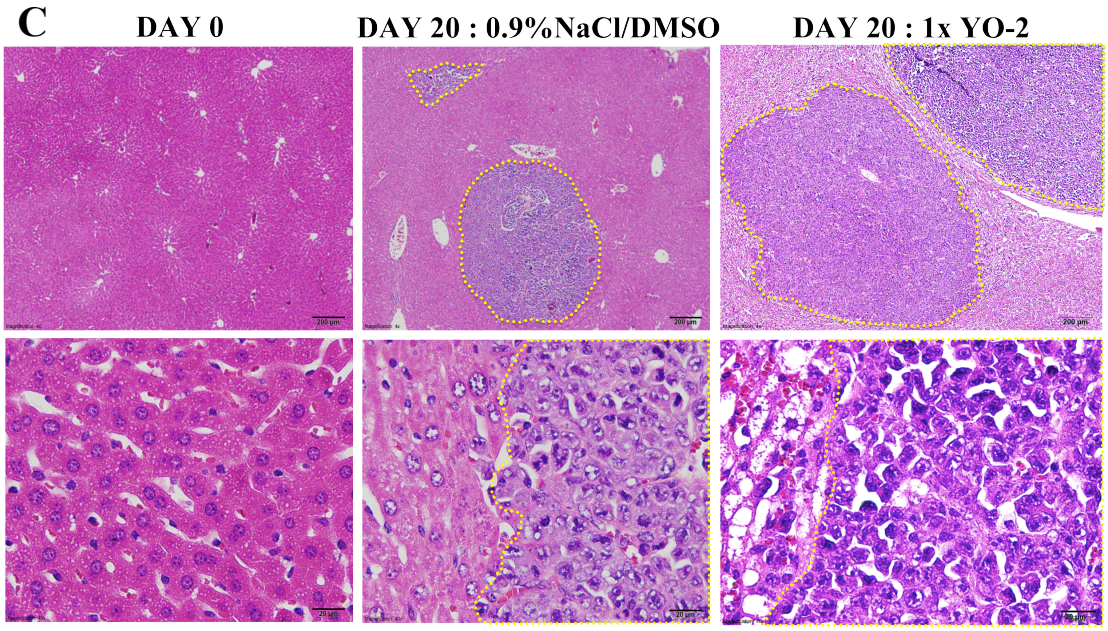

Figure 16: MM cell infiltration at intramedullar and extramedullar sites in murine syngeneic B53 MM model. Representative images of hematoxylin and eosin (H&E) from **(A)** bone marrow section (scale bar, 20 µm) **(B)** spleen (scale bar, 100 µm (above) and 20 µm (below), and **(C)** liver (scale bar, 200 µm (above) and 20 µm (below). Dotted lines indicate B53 tumor infiltrations in the different organs.

To confirm BM infiltration, which is one of the main features found in MM patients, FACS analysis was performed. The cell surface marker $H2K^{d+}$, $H2K^{b-}$ and $CD138^{+}$ were used to discriminate B53 cells from host cells, which express $H2K^{d+}$ and $H2K^{b+}$ antigen. FACS analysis showed a varying number of infiltrating B53 cells in the BM (Figure 17A). Concomitant with the infiltration of MM cells into the BM cavity, the total number of BMMNCs decreased (Figure 17B).

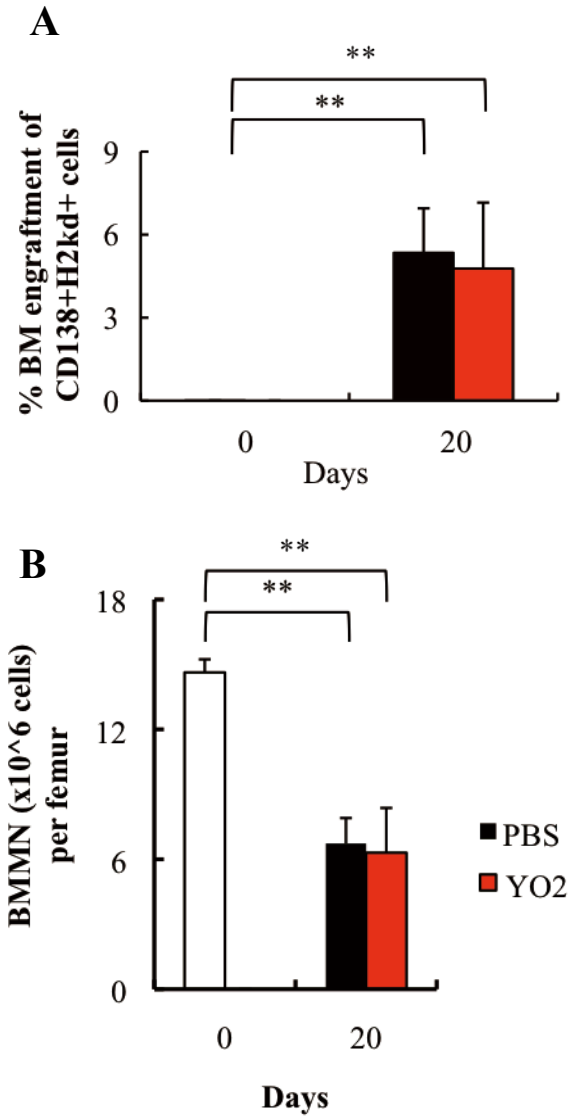

Figure 17: Decreased BM cellularity in B53 injected mice. After BM cell flushing, BMMNCs were co-stained with antibodies against CD138 and $H2k^{d}$, and the percentage of **(A)** $H2k^{d+}$ $CD138^{+}$ cells was determined by FACS (n = 3 per group). **(B)** BMMNCs were counted per femur at indicated groups. Data are represented as mean ± SEM. $^{**}p \leq 0.02$.

Due to the high variation in the tumor cell infiltration into organs between individual mice, tumor infiltration could not be used to assess the effectiveness of YO-2 treatment. Following tumor transplantation, some mice from all groups developed hind-limb paralysis, but did not develop osteolytic lesions as seen by micro-X ray analysis (Figure 18).

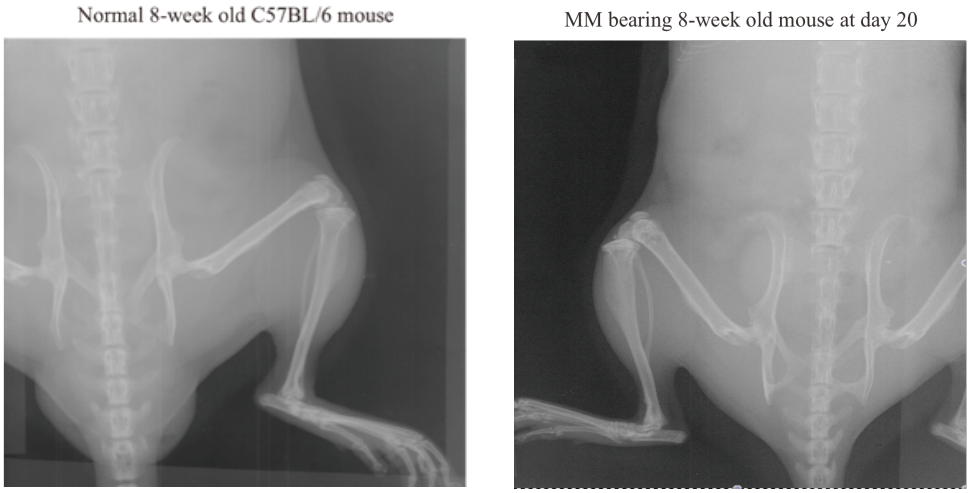

Figure 18: No osteolytic lesions in B53-injected mice. Micro-X ray images were taken on day 20 from B53-injected mice (n = 3 mice per group analyzed). No osteolysis was found in MM-bearing mice **(right)** when compare to normal group **(left)** (representative photograph).

The detection of immunoglobulin, anti-DNP IgE plasma levels released by B53 MM cells is a good marker to estimate the tumor load and to monitor disease progression in the B53 MM model. In circulation, anti-DNP IgE plasma levels increased from day 0 until day 20 (Figure 19A). Aside from the determination of IgE levels, the most reliable parameter to judge MM progression was mouse survival (Figure 19B). YO-2 could not rescue the dead or reduce the tumor burden in tumor bearing mice.

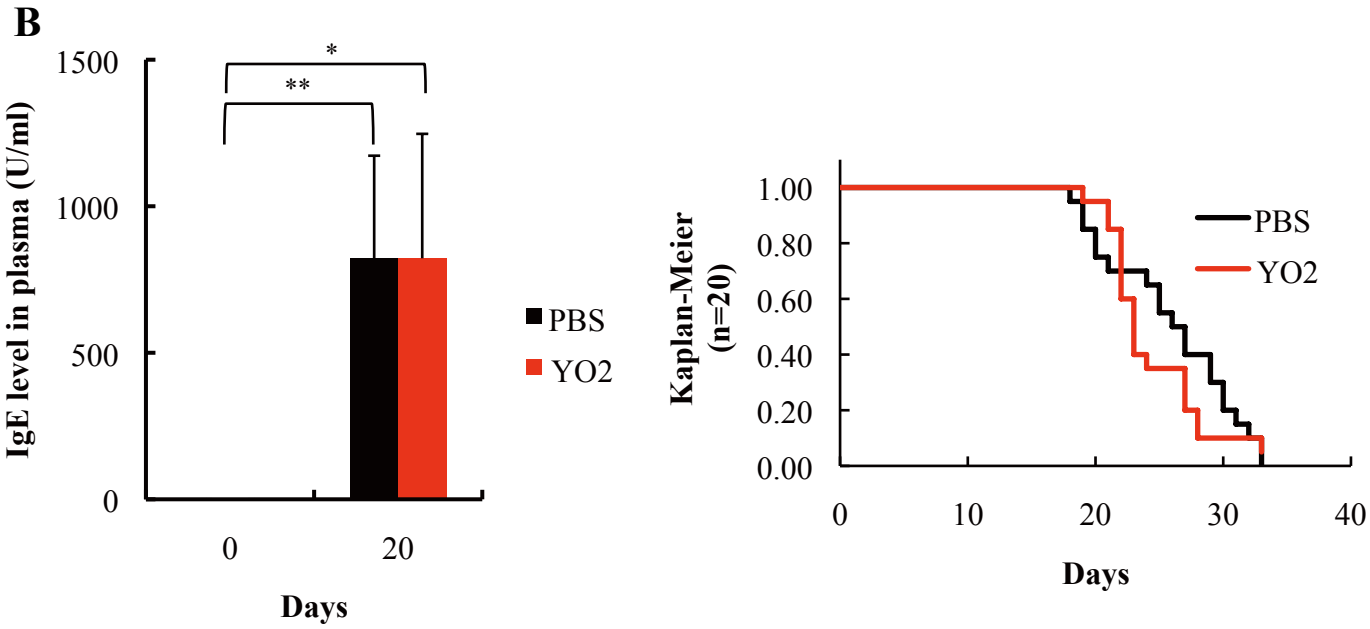

Figure 19: ***Tumor burden as measured by paraprotein IgE levels and survival*** **in YO-2 and PBS treated B53 injected mice. (A)** Paraprotein IgE levels in the plasma at day 0 and at day 20 of B53-bearing mice. **(B)** Survival curve of myeloma-bearing mice treated with PBS or YO-2. n = 20 per group. Data are represented as mean ± SEM. $^{**}p \leq 0.02$ and $^{*}p \leq 0.05$.

To test whether the non-responsiveness of YO-2 for myeloma progression in vivo might be drug specific, we tested another fibrinolytic inhibitor. Tranexamic acid (TA) is a synthetic derivative of the amino-acid lysine, which exerts its anti-fibrinolytic effect through the reversible blockade of lysine binding sites on the plm molecules. TA also could not prevent tumor growth and progression (Figure 20). Together, these data indicate that plasmin inhibitor treatment *in vivo* at 1x concentration did not alter disease progression, as determined by tissue tumor infiltration, survival and paraprotein concentration in the murine B53 MM model.

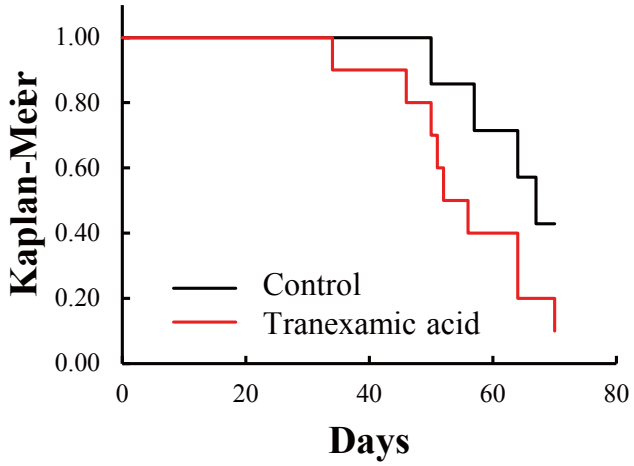

Figure 20: Anti-myeloma effect of the plasmin inhibitor tranexamic acid (TA) in B53-bearing mice. Survival curve of myeloma-bearing mice in mice treated orally with TA compared to controls. n = 10 per group.

Dose escalation and toxicity study of YO-2

Given the unresponsiveness of MM progression to YO-2 treatment, we speculated that one reason might be a suboptimal dosage of YO-2. The drug dosage was increased until signs of toxicity were visible. Increased YO-2 doses were found to be ineffective to prolong mouse survival. On the contrary, a shortened survival was observed when a dosage of 3x YO-2 (11.25 mg/kg mouse body weight) was tested (Figure 21).

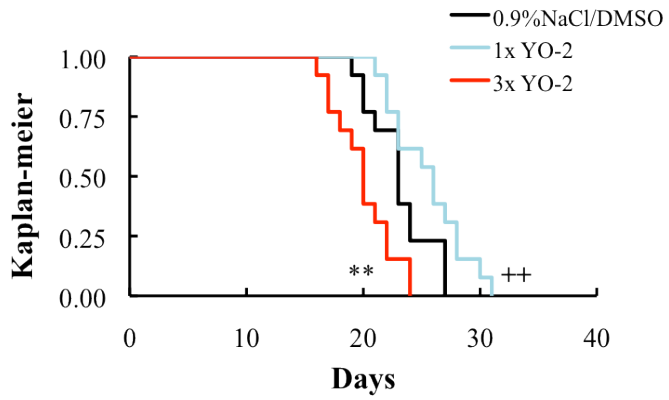

Figure 21: *In vivo* anti-myeloma effect using increasing doses of YO-2 in B53 cell bearing mice. Shortened survival was observed in 3xYO-2 treated mice, when compared to 0.9%NaCl/DMSO treated control mice and. n = 10/group. **, $^{++}$ $p \leq 0.02$, when control (0.9%NaCl/DMSO) group was compared to 1x YO-2 and 3x YO-2 groups, respectively

Even though YO-2 has been reported to inhibit plasmin and to cause apoptosis in cancer cell lines or in xenograft model [54], YO-2 treatment could not rescue the death of MM bearing mice. This might be due to the complexity of the regulation of MM cell growth *in vivo*. To study the direct effects of plm inhibition on MM cell growth *in vitro*, murine B53 and human RPMI8226 MM cells were treated with YO-2 at various concentrations for 24 hours followed by the assessment of cell viability using the trypan blue exclusion method.

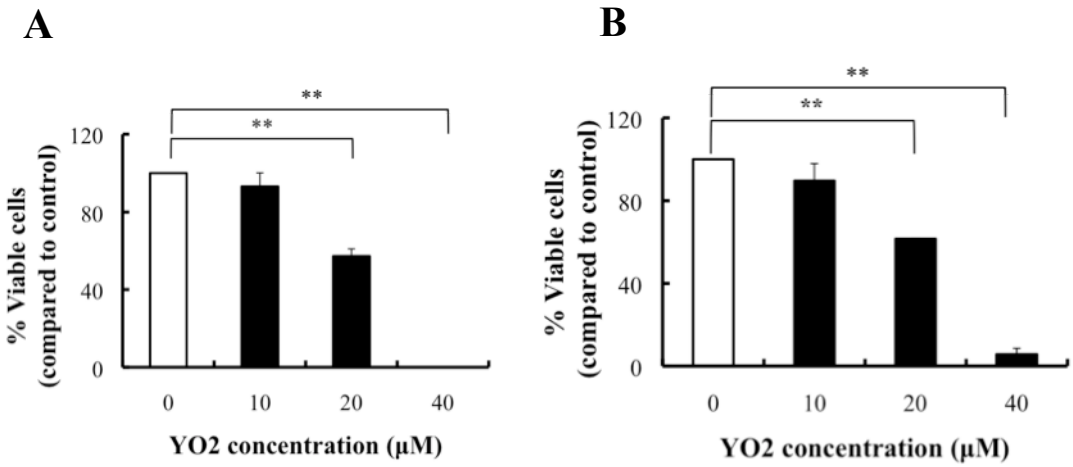

Figure 22: Dose dependent anti-myeloma effect of YO-2 *in vitro*. YO-2 (0-40 µM) was added to cultures **(A)** containing mouse MM B53 cells, or human MM RPMI8226 cells. **(B)** The IC_{50} of B53 and RPMI8226 cells was approximately 20 µM. Data are represented as mean ± SEM. $^{**}p \leq 0.02$.

Exposure to YO-2 at a concentration of 20 µM impaired the *in vitro* viability of both B53 and RPMI8226 cells (Figure 22A and B, respectively). At this concentration, YO-2 also exerted cytotoxic effects on BMMNCs and splenocytes after 12 hours (data not shown) and 24 hours with an IC_{50} of 15 µM (Figure 23A, and 23B). The human monocytic THP-1 and murine monocytic RAW264.7 cells showed an IC_{50} of 10 µM (Figure 23C and 23D). Taken together, YO-2 treatment induced cell death of not only MM cells but also of non-cancer cells like primary mouse BMMNC cells, splenocyte or monocytic cell lines, as already has been reported in thymocytes [43].

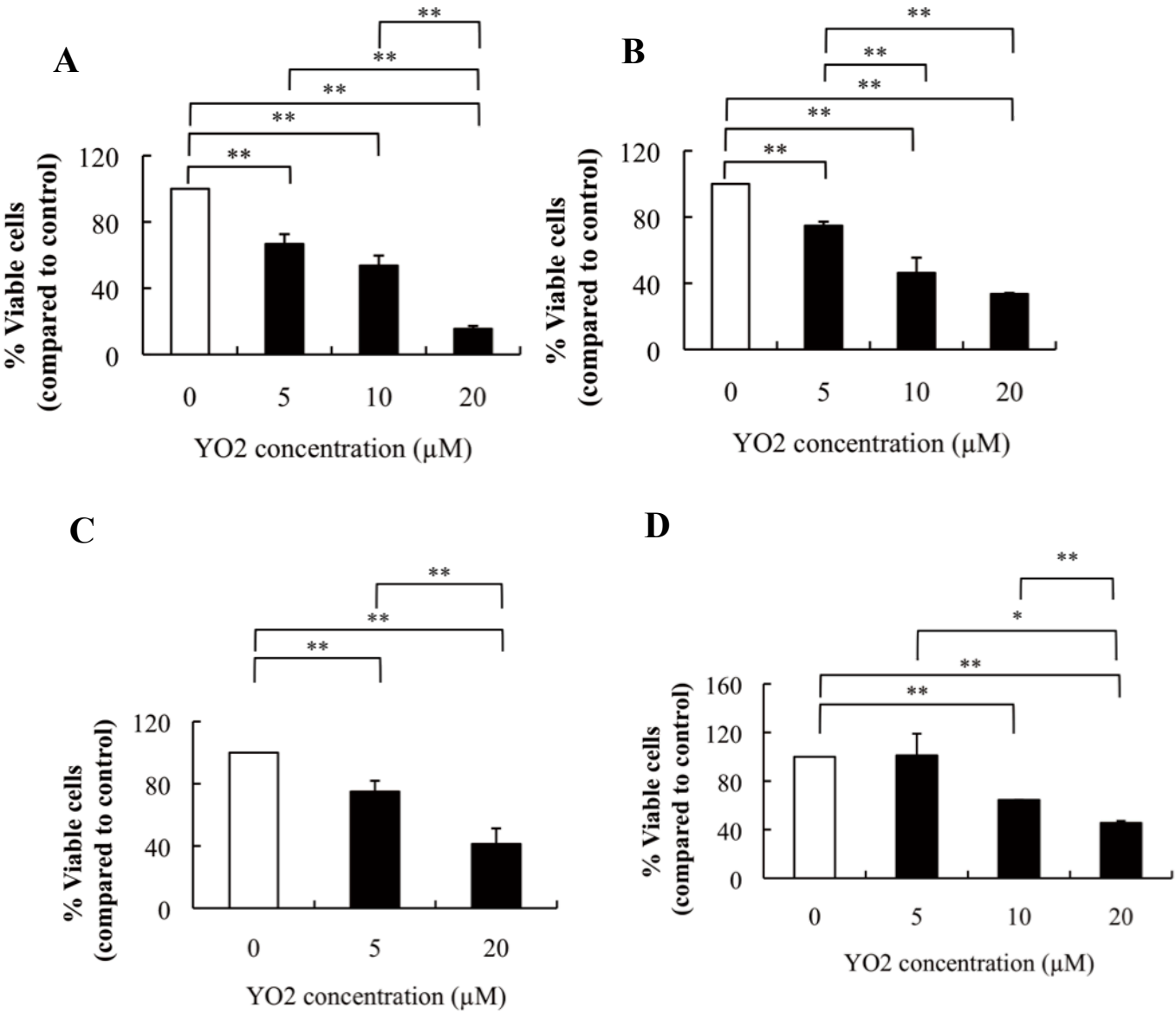

Figure 23: Viability of murine non-malignant BMMNCs and splenocytes after YO-2 exposure *in vitro*. Dose response of YO-2 (0-20 μM) on murine **(A)** BMMNCs, **(B)** splenocytes, **(C)** human monocytic THP-1, and **(D)** murine monocytic RAW264.7 cells shown as percentage compared to control group. Inhibition of cell growth was detected by trypan blue exclusion test. Data are represented as mean ± SEM. $^{**}p \leq 0.02$ and $^{*}p \leq 0.05$.

However, non-tumor CBF1 mice treated with high concentration of YO-2, a YO-2 concentration that in B53bearing mice accelerated death, did not impair survival (Figure 24A), did not decrease the number of BMMNCs (Figure 24B), or cause pathohistological abnormalities in organs observed (Figure 25).

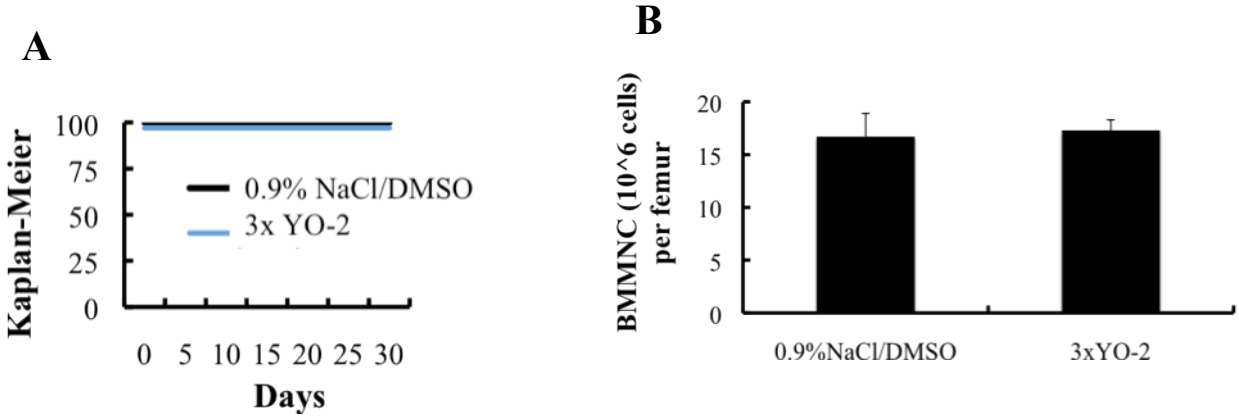

Figure 24: At high concentration (3x) YO-2 therapy did not cause the death of non-tumor bearing mice or BMMNC toxicity. (A) Survival curve of normal CBF1 mice treated with 0.9%NaCl/DMSO (control) or 3x YO-2 (n = 6 and 7, respectively). **(B)** BMMNCs were counted per femur. Data are represented as mean ± SEM

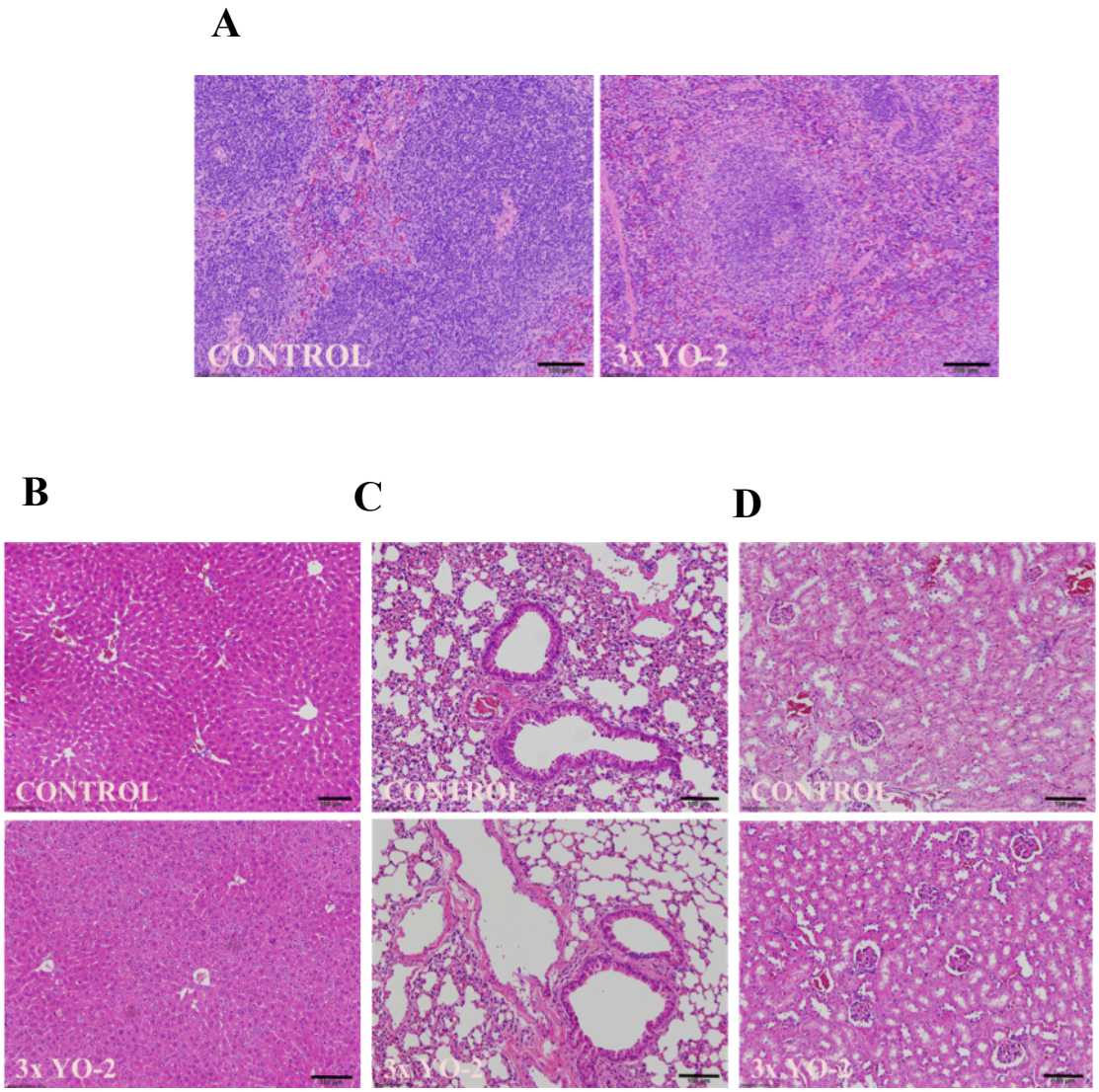

Figure 25: No macroscopical changes in tissues of non-tumor bearing mice after high dose treatment with YO-2. Representative images of hematoxylin and eosin (H&E) of **(A)** spleen (scale bar, 100 µm) **(B)** liver (scale bar, 100 µm), **(C)** lung (scale bar, 100 µm) and **(D)** kidney (scale bar, 100 µm) sections are shown.

UNDISCLOSED

Due to special circumstance

UNDISCLOSED

Due to special circumstance

UNDISCLOSED

Due to special circumstance

UNDISCLOSED

Due to special circumstance

YO-2 treatment does not suppress MM cell growth in s.c. xenograft RPMI8226 MM model

To investigate the effect of plasmin inhibition in another *in vivo* MM model, we examined the efficacy of YO-2 in the xenograft RPMI8226 MM model (Figure 29). NOD-SCID mice were inoculated subcutaneously with luciferase-tagged RPMI8226 cells and treated with/without YO-2. Subcutaneous tumor growth was monitored by determining immunofluorescence signal (Figure 29C) and by measuring the tumor size (Figure 29D). No difference in tumor growth was found when comparing YO-2-treated and PBS-treated mice. No plasma elevation of active plm was detectable in both YO-2-treated and untreated groups in this s.c. MM model (Figure 29B).

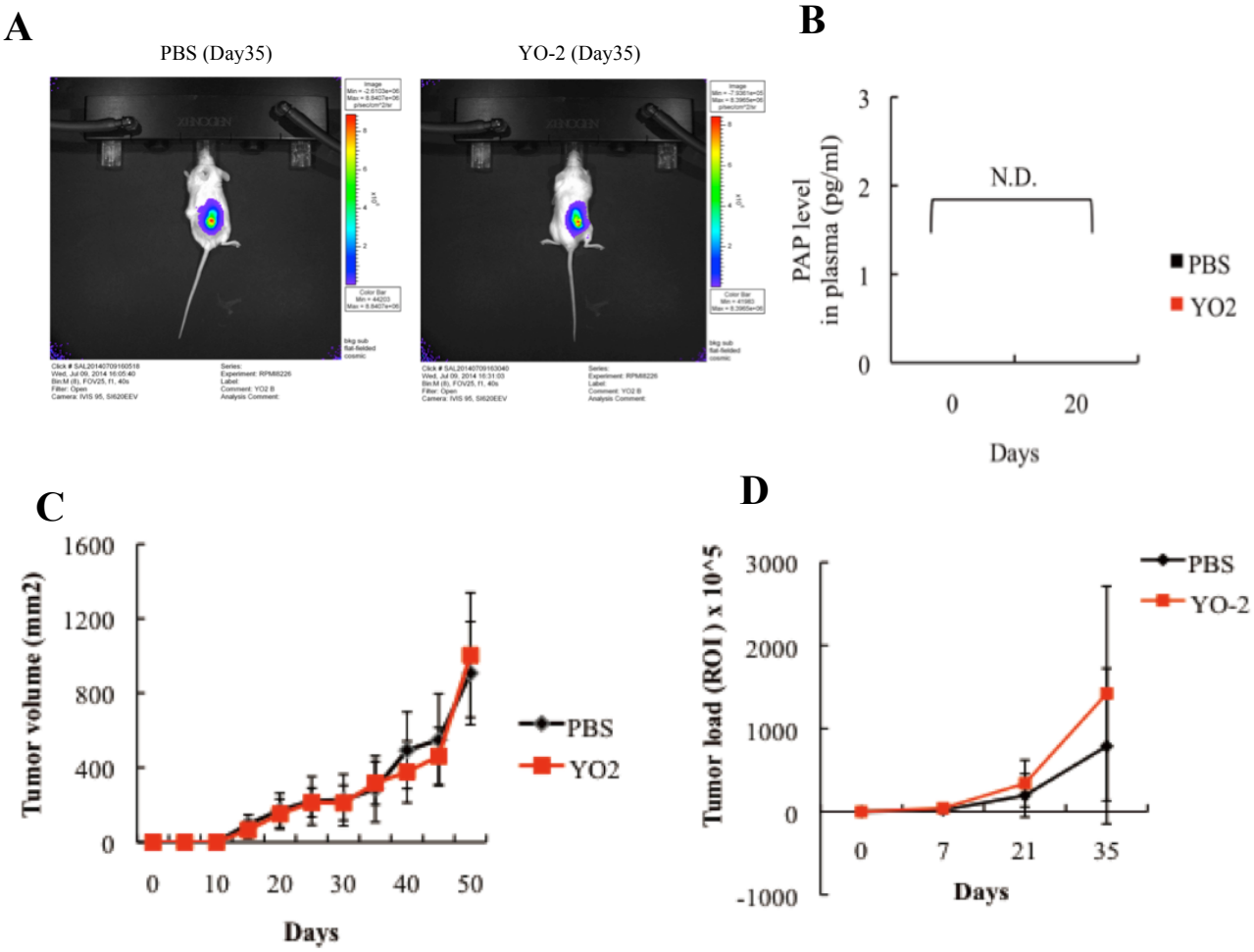

Figure 29: Tumors progress at a similar speed in control (PBS) and YO-2-treated mice. NOD/SCID mice were injected subcutaneously with 1 or 4 x 10^6 luciferase-tagged human RPMI8226. They were treated with/without 1x YO-2. Bioluminescence imaging was acquired on day 0, 7, 21 and 35 after MM cell injection. **(A)** Luciferase signal reflecting the tumor load was monitored at different time points in control (left) and YO-2 (right)-treated mice. Tumor growth was also confirmed by measuring the tumor size by vernier caliper. **(B)** Plasma levels of PAP were determined with ELISA. **(C)** Tumor volume was quantified by size and by **(D)** luciferase signal. Data are represented as mean ± SEM.

DISCUSSION

Activation of the fibrinolytic system has been linked to disease progression in many kinds of solid tumors like prostate, ovarian, colorectal cancer, and hematological cancers. Plg deficiency reduced spontaneous metastasis without affecting tumor growth in the Polyoma virus middle T antigen (PymT)-induced mammary cancer in mouse model [57], and uPA deficiency *in vivo* suppressed the formation of lung and lymph node metastasis [58].

Increased levels of fibrinolytic factors in plasma have been reported in MM patients. MM cells isolated from patients express the fibrinolytic factors, uPA and uPAR [6]. It was speculated that the activation of the fibrinolytic pathway might be associated with the degradation of the bone matrix in MM [6] and plasminogen/plasmin can contribute to bone metabolism as proved in $plg^{-/-}$ mice [59]. The current research attempted to study the involvement of the fibrinolytic factors in the biology of MM.

Myeloma cell survival and proliferation are regulated by the interaction of myeloma cells with BM microenvironmental cells. In some cancers, the interaction between cancer cells and stromal fibroblasts could activate the uPA/plasmin cascade and was linked to metastatic behavior [60]. We demonstrated that human and murine stromal, but not MM cell lines show high levels of fibrinolytic factors. Only the murine plasmocytoma B53 cell line expressed uPA and uPAR. The B53 cell line was selected for further studies because these cells showed a similar expression pattern to the one found on human primary MM cells and also showed responsiveness to common anti-myeloma drugs.

To study the involvement of fibrinolytic factors *in vivo*, a murine syngeneic MM model was established by injecting the B53 plasmacytoma cells intravenously into CBF1 mice. This B53 MM model showed some benefits compared to other mouse MM models: (1) the cross-species related problems can be avoided due to the syngeneic nature of the model. (2) The mouse model does not require irradiation. Furthermore, the MM recipients are immune-competent mice allowing us to study the effects of MM cell growth on immune cells [61]. Moreover, (3) B53 cells were able to home to the BM and infiltrate into extramedullar organs like spleen and liver. MM cell infiltration into the BM is rarely observed in other mouse models of MM, but it is a critical clinical feature of human MM disease and MM pathogenesis [62]. Therefore, the murine B53 MM model represents as an attractive model to study the interactions of myeloma cells with BM stromal cells or MM infiltration. It is also an ideal mouse model for pre-clinical drug testing, because (4) the disease progresses quickly after initial tumor

cell inoculation and (5) disease progression can be monitored by parameters like circulating IgE levels and mouse survival [62]. Finally, the decrease in BM cellularity was observed in B53 injected mice, indicating that B53 cell expansion in BM had affected the normal blood cell proliferation, a well-known phenomenon found in MM patients.

Osteolysis requires the interaction of stromal cells and MM cells. But no macroscopically visible osteolytic lesions were observed by X-ray in B53 injected mice. The lack of macroscopical osteolytic lesions in the B53 model could be explained by the fact that B53 cells may not require adhesion to stromal cells, which is necessary for the induction of osteolytic mechanism-related factors. Studies showed that plasmin activators are not required for osteoclast formation or bone resorption in the mineral phrase of bone formation, and are only involved in the degradation of noncollagenous matrix proteins [63].

In contrast to a report [39], high levels of circulating plasmin-anti plasmin were found in our newly established syngeneic B53 MM model, indicating that most likely in a disease phase-dependent manner, the activation of the fibrinolytic system occurs. These data prompted us to investigate the effects of the plm inhibitor YO-2, a drug that blocks active plm, on tumor progression.

It was reported that YO-2 treatment blocked tumor growth in human tumor xenograft models (e.g. the human HT-29 colon carcinoma and HT-58 B cell lymphoma) at effective treatment doses between 0.4-4 mg/kg [54]. Here, we treated B53 bearing mice with YO-2 at a concentration of 3.75 mg/kg which is a dose that we previously reported to be effective in controlling the progression of murine T cell lymphoma, and inflammatory diseases like acute graft versus host disease and inflammatory bowel disease [41, 44, 64].

However, at this dose, YO-2 could not block MM disease progression *in vivo* and the circulating active plasmin was not completely suppressed. We questioned whether the failure in controlling tumor growth was due to a non-sufficient dosage of YO-2. The dose of YO-2 was escalated with concentration from 3.75 mg/kg to 7.5, 11.25 and 15 mg/kg, referred as 1x, 2x, 3x and 4x, respectively (Data of YO-2 treatment with 2x and 4x doses are not shown). Of interest, high doses of YO-2 (3x and 4x) significantly accelerated tumor progression and death in MM bearing mice but surprisingly no toxicity was observed in normal CBF1 mice treated with high concentration of YO-2 (3x).

One of the possibilities for the increased death rate at high doses of YO-2 could be that YO-2 boosts the tumor growth *in vivo*. Another possibility could be that YO-2 increases the risk of thrombosis and thrombus-related death. However, these hypotheses are unlikely because we observed (1) no difference in IgE plasma levels and (2) no macroscopically detectable thrombosis in mouse organs comparing mice treated with YO-2 at 1x or 3x. The reason why high concentration of YO-2 accelerated the death in MM bearing mice only is still unclear, and requires further investigations. To determine whether the failure to control MM growth was a YO-2-specific drug effect, tranexamic acid (TA), another plasmin inhibitor, was investigated. Similar to YO-2, TA treatment also could not block MM growth *in vivo*.

MM is a disease associated with high risk of venous and arterial thromboembolism [61]. Hypofibrinolysis with increased PAI-1 levels may cause a prothrombotic state [53]. Yagci et al. reported an increase of PAI-1 and proposed that MM should be considered as a disease with hypercoagulation [39, 65]. The natural response of the body to thrombosis is the activation of the fibrinolytic system [66]. While high levels of PAI-1 (endogenous inhibitor of PA) in MM patients were reported [39], uPA, uPAR or suPAR, which are components of fibrinolytic system are augmented in MM patients [6, 30]. This could imply that there is a phase-dependent activation of fibrinolysis and thrombosis. Due to the anti-apoptotic properties of PAI-1 in various cell types, future studies will need to address whether PAI-1 inhibitor treatment can control MM cell growth.

YO-2 can induce apoptosis by activating caspase-3, -8, -9 as reported in cancer cell lines, and thymocytes [41-43]. We showed that YO-2 could induce apoptosis in murine B53 and human RPMI8226 cell lines in a concentration-dependent manner *in vitro*, but also induced cell death in primary mouse cells and the monocytic cell lines THP-1 and RAW264.7. Although *in vitro* toxicity was observed, no systemic toxicity had been reported by our group or others using YO-2 *in vivo* in other murine cancer models [41, 54]. The reason for differences in apoptosis induction observed *in vitro* but not *in vivo* might be in part due to the activation of compensatory pathways *in vivo*, e.g. the protective stromal niche in which MM cells reside.

Next, we used a well-known established xenograft RPMI8226 MM model where the inoculated MM cells localize at the injection area and dissemination did not occur. No systemic increase in plasmin was observed during disease progression. YO-2 treatment could not control tumor progression in this MM model either.

Although the fibrinolytic system is activated during the early phase of B53 bearing murine model, the disease progression could not be prevented using pharmacological blockade of plasmin inhibitor YO-2. This could be due to the incomplete plasmin-inhibiting effect of YO-2 and the limitation of dose usage. The successful treatment of YO-2 in another disease model could be explained by the fact that circulating plasmin level was significantly decreased after YO-2 treatment when compared to non-treated group, resulting in being able to rescue the death of the mice [44, 64]. However, in our MM mouse model, even though there was a trend in the decrease of plasmin level but it was not enough to be significant between treated and non-treated group. The aggressiveness of B53 cells is suspected for the unresponsiveness of YO-2.

In this B53 model, tumor burden developed very fast and all mice died in less than 40 days. Although YO-2 could inhibit B53 proliferation *in vitro*, it could not impair B53 proliferation *in vivo*. The tumor growth control potential of YO-2 in other tumor disease models might be due to the fact that other tumors grow at a lower growth rate - which is in contrast to our MM model. Due to B53 aggressiveness, other solid tumors may be less dependent on microenvironmental cells, including stromal cells, which are the main source of fibrinolytic factors, or myeloid cells, which is a novel downstream target of plasmin [44, 64].

It is possible that less aggressive models of MM or the inoculation of a smaller cell number might indeed show that YO-2 can control tumor growth under these conditions. Further studies will be necessary to determine the effect of YO-2 under these conditions. Due to a long-term maintenance of the cells in culture for more than 6 months, we accidentally established B53 cells that showed a lower proliferation rate and were less aggressive when injected in mice. These cells showed a lower expression of the cell surface marker $H2k^d$ when compared to the newly thawed mother B53 cells (data not shown), and the observed reduced expression of $H2k^d$ might have resulted in a higher allograft rejection of the cells. But even in this less aggressive model of MM, YO-2 treatment could not alter the disease progression.

In conclusion, YO-2 could not only completely inhibit the upregulation of plasmin in B53 bearing mice, but rather accelerated the death of tumor bearing mice when the doses were escalated. However it is very interesting that the high dose toxicity did not cause side effect in normal mice. The explanation for what YO-2 does on tumor *in vivo* still needs to be clarified and further investigated.

REFERENCES

1. Palumbo A, Anderson K. Multiple myeloma. N Engl J Med 2011;364:1046-60.
2. Balakumaran A, Robey PG, Fedarko N, et al. Bone marrow microenvironment in myelomagenesis: its potential role in early diagnosis. Expert Rev Mol Diagn 2010;10:465-80.
3. Kyle RA. Multiple myeloma: an odyssey of discovery. Br J Haematol 2000;111:1035-44.
4. Tete SM, Bijl M, Sahota SS, et al. Immune defects in the risk of infection and response to vaccination in monoclonal gammopathy of undetermined significance and multiple myeloma. Front Immunol 2014;5:257.
5. Van Valckenborgh E, Croucher PI, De Raeve H, et al. Multifunctional role of matrix metalloproteinases in multiple myeloma: a study in the 5T2MM mouse model. Am J Pathol 2004;165:869-78.
6. Hjertner O, Qvigstad G, Hjorth-Hansen H, et al. Expression of urokinase plasminogen activator and the urokinase plasminogen activator receptor in myeloma cells. Br J Haematol. 2000;109:815-22.
7. Kawano Y, Moschetta M, Manier S, et al. Targeting the bone marrow microenvironment in multiple myeloma. Immunol Rev 2015;263:160-72.
8. Hideshima T, Bergsagel PL, Kuehl WM, et al. Advances in biology of multiple myeloma: clinical applications. Blood 2004;104:607-18.
9. Morgan GJ, Walker BA, Davies FE. The genetic architecture of multiple myeloma. Nat Rev Cancer 2012;12:335-48.
10. Heissig B, Lund LR, Akiyama H, et al. The plasminogen fibrinolytic pathway is required for hematopoietic regeneration. Cell Stem Cell 2007;1:658-70.
11. Podar K, Hideshima T, Chauhan D, et al. Targeting signalling pathways for the treatment of multiple myeloma. Expert Opin Ther Targets. 2005;9:359-81.
12. Deora AB, Kreitzer G, Jacovina AT, et al. An annexin 2 phosphorylation switch mediates p11-dependent translocation of annexin 2 to the cell surface. J Biol Chem 2004;279:43411-8.
13. Seckinger A, Meissner T Fau - Moreaux J, Moreaux J Fau - Depeweg D, et al. Clinical and prognostic role of annexin A2 in multiple myeloma.
14. Bao H, Jiang M Fau - Zhu M, Zhu M Fau - Sheng F, et al. Overexpression of Annexin II affects the proliferation, apoptosis, invasion and production of proangiogenic factors in multiple myeloma.
15. Heissig B, Eiamboonsert S, Salama Y, et al. Cancer therapy targeting the fibrinolytic system. Adv Drug Deliv Rev 2015.
16. Barille S, Akhoundi C, Collette M, et al. Metalloproteinases in multiple myeloma: production of matrix metalloproteinase-9 (MMP-9), activation of proMMP-2, and induction of MMP-1 by myeloma cells. Blood. 1997;90:1649-55.
17. Jourdan M, Tarte K, Legouffe E, et al. Tumor necrosis factor is a survival and proliferation factor for human myeloma cells. Eur Cytokine Netw 1999;10:65-70.
18. Zhang XG, Gu JJ, Lu ZY, et al. Ciliary neurotropic factor, interleukin 11, leukemia inhibitory factor, and oncostatin M are growth factors for human myeloma cell lines using the interleukin 6 signal transducer gp130. J Exp Med 1994;179:1337-42.
19. Vacca A, Ria R, Semeraro F, et al. Endothelial cells in the bone marrow of patients with multiple myeloma. Blood 2003;102:3340-8.
20. Lyons RM, Gentry LE, Purchio AF, et al. Mechanism of activation of latent recombinant transforming growth factor beta 1 by plasmin. J Cell Biol 1990;110:1361-7.
21. Campbell PG, Novak JF, Yanosick TB, et al. Involvement of the plasmin system in dissociation of the insulin-like growth factor-binding protein complex. Endocrinology 1992;130:1401-12.
22. Carmeliet P, Moons L, Lijnen R, et al. Urokinase-generated plasmin activates matrix metalloproteinases during aneurysm formation. Nat Genet 1997;17:439-44.
23. Rifkin DB, Mazzieri R, Munger JS, et al. Proteolytic control of growth factor availability. APMIS 1999;107:80-5.
24. Moses MA. The regulation of neovascularization of matrix metalloproteinases and their inhibitors. Stem Cells 1997;15:180-9.

25. Bergers G, Brekken R, McMahon G, et al. Matrix metalloproteinase-9 triggers the angiogenic switch during carcinogenesis. Nat Cell Biol 2000;2:737-44.
26. Stamenkovic I. Matrix metalloproteinases in tumor invasion and metastasis. Semin Cancer Biol 2000;10:415-33.
27. Tricot G. New insights into role of microenvironment in multiple myeloma. Lancet 2000;355:248.
28. Hecht M, von Metzler I, Sack K, et al. Interactions of myeloma cells with osteoclasts promote tumour expansion and bone degradation through activation of a complex signalling network and upregulation of cathepsin K, matrix metalloproteinases (MMPs) and urokinase plasminogen activator (uPA). Exp Cell Res. 2008;314:1082-93 Epub 2007 Nov 7.
29. Hecht M, Heider U, Kaiser M, et al. Osteoblasts promote migration and invasion of myeloma cells through upregulation of matrix metalloproteinases, urokinase plasminogen activator, hepatocyte growth factor and activation of p38 MAPK. Br J Haematol. 2007;138:446-58 Epub 2007 Jun 25.
30. Rigolin GM, Tieghi A, Ciccone M, et al. Soluble urokinase-type plasminogen activator receptor (suPAR) as an independent factor predicting worse prognosis and extra-bone marrow involvement in multiple myeloma patients. Br J Haematol. 2003;120:953-9.
31. Rasch MG, Lund IK, Almasi CE, et al. Intact and cleaved uPAR forms: diagnostic and prognostic value in cancer. Front Biosci. 2008;13:6752-62.
32. Smith HW, Marshall CJ. Regulation of cell signalling by uPAR. Nat Rev Mol Cell Biol 2010;11:23-36.
33. Jo M, Thomas KS, Wu L, et al. Soluble Urokinase-type Plasminogen Activator Receptor Inhibits Cancer Cell Growth and Invasion by Direct Urokinase-independent Effects on Cell Signaling. Journal of Biological Chemistry 2003;278:46692.
34. Seidel C, Sundan A, Hjorth M, et al. Serum syndecan-1: a new independent prognostic marker in multiple myeloma. Blood 2000;95:388-92.
35. Parmo-Cabanas M, Molina-Ortiz I, Matias-Roman S, et al. Role of metalloproteinases MMP-9 and MT1-MMP in CXCL12-promoted myeloma cell invasion across basement membranes. J Pathol 2006;208:108-18.
36. Vacca A, Ribatti D, Iurlaro M, et al. Human lymphoblastoid cells produce extracellular matrix-degrading enzymes and induce endothelial cell proliferation, migration, morphogenesis, and angiogenesis. Int J Clin Lab Res 1998;28:55-68.
37. Vacca A. Bone marrow neovascularization, plasma cell angiogenic potential, and matrix metalloproteinase-2 secretion parallel progression of human multiple myeloma. Blood 1999;93:3064.
38. Wahlgren J, Maisi P, Sorsa T, et al. Expression and induction of collagenases (MMP-8 and -13) in plasma cells associated with bone-destructive lesions. J Pathol 2001;194:217-24.
39. Yagci M, Sucak GT, Haznedar R. Fibrinolytic activity in multiple myeloma. Am J Hematol 2003;74:231-7.
40. Zangari M, Fink L, Zhan F, et al. Low venous thromboembolic risk with bortezomib in multiple myeloma and potential protective effect with thalidomide/lenalidomide-based therapy: review of data from phase 3 trials and studies of novel combination regimens. Clin Lymphoma Myeloma Leuk 2011;11:228-36.
41. Ishihara M, Nishida C, Tashiro Y, et al. Plasmin inhibitor reduces T-cell lymphoid tumor growth by suppressing matrix metalloproteinase-9-dependent CD11b(+)/F4/80(+) myeloid cell recruitment. Leukemia 2012;26:332-9.
42. Okada Y, Tsuda Y, Tada M, et al. Development of potent and selective plasmin and plasma kallikrein inhibitors and studies on the structure-activity relationship. Chem Pharm Bull (Tokyo) 2000;48:1964-72.
43. Lee E, Enomoto R, Takemura K, et al. A selective plasmin inhibitor, trans-aminomethylcyclohexanecarbonyl-L-(O-picolyl)tyrosine-octylamide (YO-2), induces thymocyte apoptosis. Biochem Pharmacol. 2002;63:1315-23.
44. Sato A, Nishida C, Sato-Kusubata K, et al. Inhibition of plasmin attenuates murine acute graft-versus-host disease mortality by suppressing the matrix metalloproteinase-9-dependent inflammatory cytokine storm and effector cell trafficking. Leukemia 2015;29:145-56.
45. Tengborn L, Blomback M, Berntorp E. Tranexamic acid--an old drug still going strong and making a revival. Thromb Res 2015;135:231-42.

46. Eubanks JD. Antifibrinolytics in major orthopaedic surgery. J Am Acad Orthop Surg 2010;18:132-8.
47. Tanaka N, Ogawa H, Kinjo M, et al. Ultrastructural study of the effects of tranexamic acid and urokinase on metastasis of Lewis lung carcinoma. Br J Cancer 1982;46:428-435.
48. Soma H, Sashida T, Yoshida M, et al. Treatment of advanced ovarian cancer with fibrinolytic inhibitor (tranexamic acid). Acta Obstet Gynecol Scand 1980;59:285-7.
49. Astedt B. Adjuvant treatment of ovarian carcinoma with tranexamic acid. J Clin Pathol Suppl (R Coll Pathol) 1980;14:74-6.
50. Enomoto R, Sugahara C, Komai T, et al. The structure-activity relationship of various YO compounds, novel plasmin inhibitors, in the apoptosis induction. Biochim Biophys Acta. 2004;1674:291-8.
51. Tsuda Y, Tada M, Wanaka K, et al. Structure-inhibitory activity relationship of plasmin and plasma kallikrein inhibitors. Chem Pharm Bull (Tokyo) 2001;49:1457-63.
52. Bottcher I, Ulrich M, Hirayama N, et al. Production of monoclonal mouse IgE antibodies with DNP specificity by hybrid cell lines. Int Arch Allergy Appl Immunol 1980;61:248-50.
53. Misiewicz M, Robak M, Chojnowski K, et al. [Correlations between ROTEM fibrinolytic activity and t-PA, PAI-1 levels in patients with newly diagnosed multiple myeloma]. Pol Merkur Lekarski 2014;36:316-9.
54. Szende B, Okada Y, Tsuda Y, et al. A novel plasmin-inhibitor inhibits the growth of human tumor xenografts and decreases metastasis number. In Vivo. 2002;16:281-6.
55. Enomoto R, Sugahara C, Tsuda Y, et al. Thymocyte apoptosis induced by various compounds including YO-2 is accompanied by a change in chromatin structure. Ann N Y Acad Sci. 2004;1030:622-6.
56. Richardson PG, Hideshima T, Mitsiades C, et al. The emerging role of novel therapies for the treatment of relapsed myeloma. J Natl Compr Canc Netw 2007;5:149-62.
57. Bugge TH, Lund LR, Kombrinck KK, et al. Reduced metastasis of Polyoma virus middle T antigen-induced mammary cancer in plasminogen-deficient mice. Oncogene 1998;16:3097-104.
58. Almholt K, Lund LR, Rygaard J, et al. Reduced metastasis of transgenic mammary cancer in urokinase-deficient mice. Int J Cancer 2005;113:525-32.
59. Kanno Y, Ishisaki A, Kawashita E, et al. Plasminogen/plasmin modulates bone metabolism by regulating the osteoblast and osteoclast function. J Biol Chem 2014;289:15154-15154.
60. He Y, Liu XD, Chen ZY, et al. Interaction between cancer cells and stromal fibroblasts is required for activation of the uPAR-uPA-MMP-2 cascade in pancreatic cancer metastasis. Clin Cancer Res 2007;13:3115-24.
61. Gado K, Silva S, Paloczi K, et al. Mouse plasmacytoma: an experimental model of human multiple myeloma. Haematologica 2001;86:227-236.
62. Fryer RA, Graham TJ, Smith EM, et al. Characterization of a novel mouse model of multiple myeloma and its use in preclinical therapeutic assessment. PLoS One 2013;8:e57641.
63. Daci E, Verstuyf A, Moermans K, et al. Mice lacking the plasminogen activator inhibitor 1 are protected from trabecular bone loss induced by estrogen deficiency. J Bone Miner Res 2000;15:1510-6.
64. Munakata S, Tashiro Y, Nishida C, et al. Inhibition of plasmin protects against colitis in mice by suppressing matrix metalloproteinase 9-mediated cytokine release from myeloid cells. Gastroenterology 2015;148:565-578 e4.
65. Undas A, Zubkiewicz-Usnarska L, Helbig G, et al. Altered plasma fibrin clot properties and fibrinolysis in patients with multiple myeloma. Eur J Clin Invest 2014;44:557-66.
66. Booth NA. Fibrinolysis and thrombosis. Baillieres Best Pract Res Clin Haematol 1999;12:423-33.

ACKNOWLEDGEMENT

I would like to spend a little space here to convey my deep sense to gratitude and respect to many people who support me. Without them, I am sure that I could not have come this far.

Firstly, I would like to dedicate this page to my supervisor, Dr. Beate Heissig, and Dr. Koichi Hattori for their understanding, their great patience, helpful advice and guidance to me. I believe that they have a good will to make us grow so we can leave from their wings and fly.

I would like to share my success with all of my lab members, especially Dr. Sato Aki, Dr. Nishida Chiemi, Mrs. Okunuki Kazuko, Mrs. Ueno Yoko, Ms. Hiroko Shimazu and Mrs. Ishii Yumiko from FACS core lab. I feel I am blessed to know these wonderful people. I also would like to thank to Mr. Yousef Salama and other lab members. I deeply appreciate their good benevolence and kind support they always give to me unlimited. A special thank to Prof. Watarai Hiroshi. I really appreciate his unconditional kindness.

I would like to say the following sentences to Douaa Dhahri, my little lab mate. I am impressed how she conducts herself. She is like the prayer as the way she is named for me. She inspires me. She is one of the people who cheers me up when I am depressed. I would like to say thanks for dragging me with her to reach the finish line, our goal. I am thankful to her for always being beside me.

Furthermore, I would like to express great thanks to Thai Government for providing me a great opportunity to study here. Now I am trying to improve myself to be good enough and I hope in the future I can contribute more or less to help improve our beloved country.

I could not find words to express enough gratitude to my parents, my brother, and S. Yuma. I strongly believe that they would be by my side no matter what will happen. Being away from home makes me realize that they love me without any condition and are always ready to support me.

Last but not least, I would like to say thank you to everyone who passed through my life here in Japan. It is such a great memory. Everyone colors my everyday!

"Bloom where you are planted"